

Structural Analysis for Fracture Optimization*

Catalina Luneburg¹, Bob Ratliff¹, and Alex Page¹

Search and Discovery Article #41728 (2015)**

Posted November 30, 2015

*Adapted from oral presentation given at 2015 AAPG Convention & Exhibition, Denver, Colorado, May 31-June 3, 2015.

**Datapages © 2015 Serial rights given by author. For all other rights contact author directly.

¹Geology, Landmark Software, Halliburton, Highlands Ranch, Colorado (Catalina.Luneburg@halliburton.com)

Abstract

In this article we present an innovative multi-disciplinary workflow based on a structural modeling technique, 'Complex Geometry fields,' that enables a geologist to generate attribute predictors for fracture densities, such as detailed bedding geometry, curvature, dip, and strain across an asset or basin. We explain and demonstrate how this technique can be used to benefit the operators of unconventional assets in the following way: the attribute predictors can be used to 'map out' an estimate of the fracture density distributions in three dimensions in a study area, which, in turn, can be used to optimally orient laterals well sections. The orientation of the laterals well sections with respect to the best estimate of the natural fracture orientation trends is thought to be of critical importance when designing completions and induced hydraulic fracture operations that ultimately control the flow of hydrocarbons into the well bore and thence to surface facilities. The computations to generate these geometry fields and predictors are based on the geometry of interpreted surfaces using established kinematic models, such as vertical/oblique shear and flexural slip that account for compressional or extensional tectonic regimes and also the geomechanical lithological competency of the target formations. A good understanding of the structural components of the basin architecture is critical not just for hydrocarbon maturity but also in terms of understanding the behavior or natural and induced fracturing and faulting. After the structural geology attributes have been computed, this information is then combined with and calibrated to other useful information, such as 3D azimuthal seismic attributes or petrophysical and geomechanical observations derived from well locations to give the highest degree of accuracy with respect to predicting the gross distribution of the regional stress state and, therefore, understanding the associated development of fracture densities. The applications of creating a multi-disciplinary 3D numerical model of the subsurface that is enriched with this regional structural geology component are

wide-reaching, but they really benefits completion and hydraulic fracturing design as well as full field well planning strategies and the associated logistics because a high fidelity prediction of the subsurface has been generated across an entire asset.

Selected References

Fox, J.E., G.L. Dolton, and J.L. Clayton, 1991, Powder River Basin, *in* H.J. Gluskoter, D.D. Rice, and R.B. Taylor, editors, Economic Geology, U.S.: Geological Society of America, The Geology of North America, P-2, p. 373-390.

Stearns, D.W., 1967, Certain aspects of fracture in naturally deformed rocks, *in* R.E. Rieker, editor, NSF Advanced Science Seminar in Rock Mechanics: Bedford, Air Force Cambridge Research Laboratories, p. 97-118.

Stearns, D.W., 1971, Mechanisms of drape folding in the Wyoming Province, *in* A.R. Renfro, L.W. Madison, G.A. Jarre, and W.A. Bradley, editors, Symposium on Wyoming tectonics and their economic significance: Twenty-Third Annual Field Conference Guidebook, Wyoming Geological Association, p. 125-143.

Stearns, D.W., 1978, Faulting and forced folding in the Rocky Mountains foreland, *in* V. Matthews, III., editor, Laramide folding associated with basement block faulting in the western United States: Geological Society of America Memoir 151, p. 1-37.

Twiss, R.J., and E.M. Moores, 1992, Structural Geology: W.H. Freeman & Company, New York, 532p.



HALLIBURTON

Landmark

STRUCTURAL ANALYSIS FOR FRACTURE OPTIMIZATION

Catalina Luneburg, Bob Ratliff and Alex Page

Landmark, Halliburton

HALLIBURTON | Landmark



Natural fractures significantly influence the hydraulic behavior of fractured reservoirs – production is enhanced in areas of high fracture density



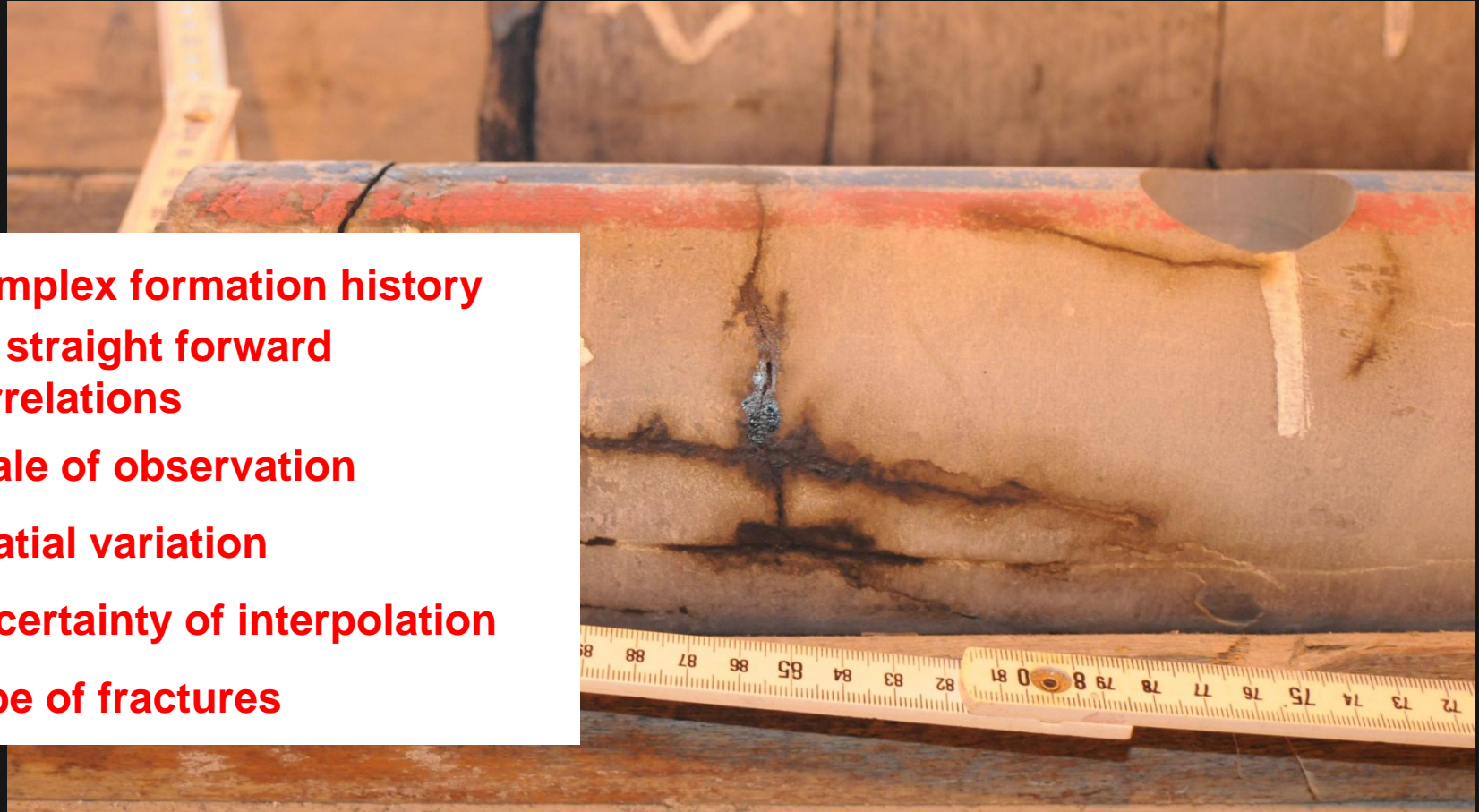
Important to quantitatively characterize and model the geometry of natural fracture systems using direct or indirect (proxies) methods



Predicting fracture geometry and density is critical for reservoir development and production forecasting, and optimizing well trajectories and drilling



Fractures critical in rocks with very low primary porosity by providing secondary porosity and permeability



- **Complex formation history**
- **No straight forward correlations**
- **Scale of observation**
- **Spatial variation**
- **Uncertainty of interpolation**
- **Type of fractures**

Well bore with oil seeps along fractures

How are fractures related to deformation?

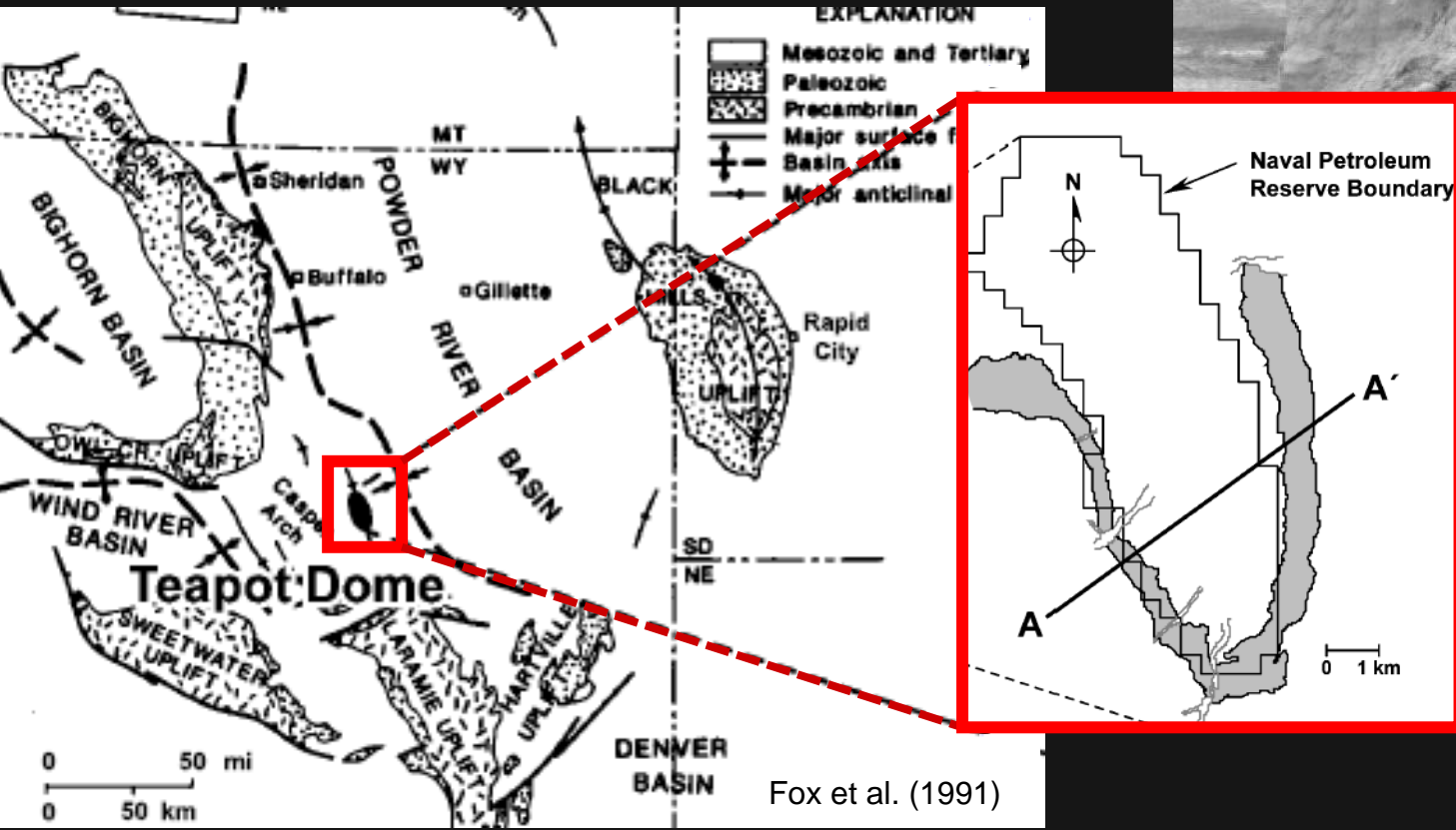
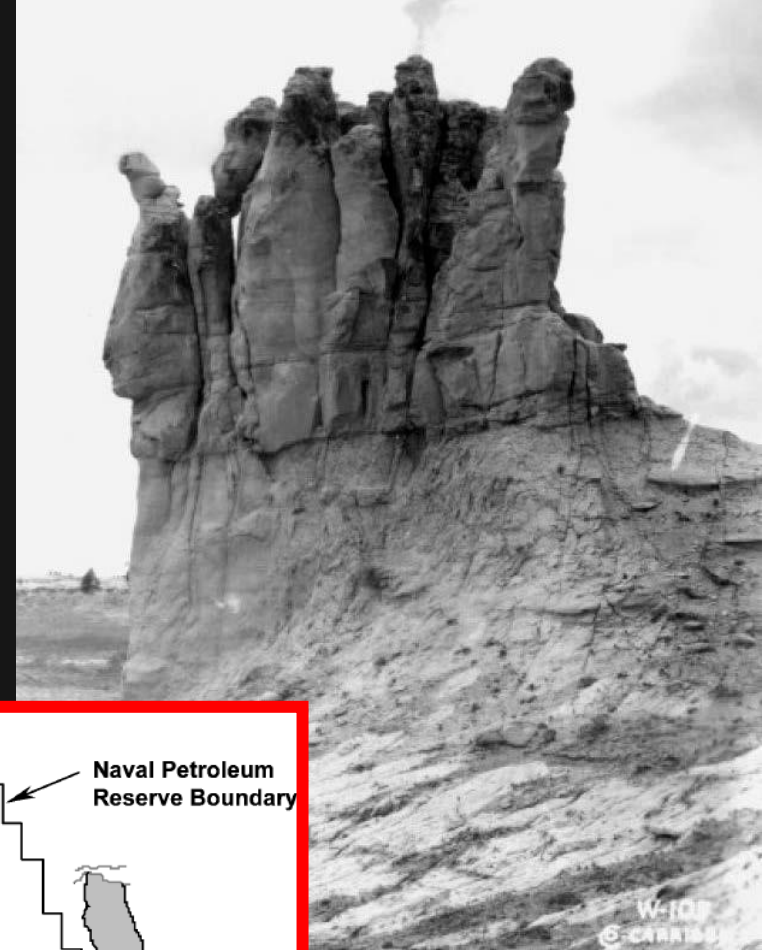
Can structural analysis provide clues to fracture intensity distribution?

Can strain be used as a fracture proxy?



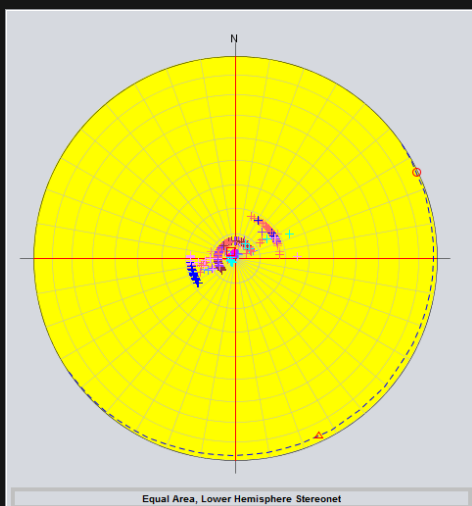
Teapot Dome, WY

- Southwestern margin of Powder River Basin WY, Laramide age foreland basin
- Unconventional fractured reservoir
- Naval Petroleum Reserve (1915) and RMOTC (1977) - recently sold



Teapot Dome, WY

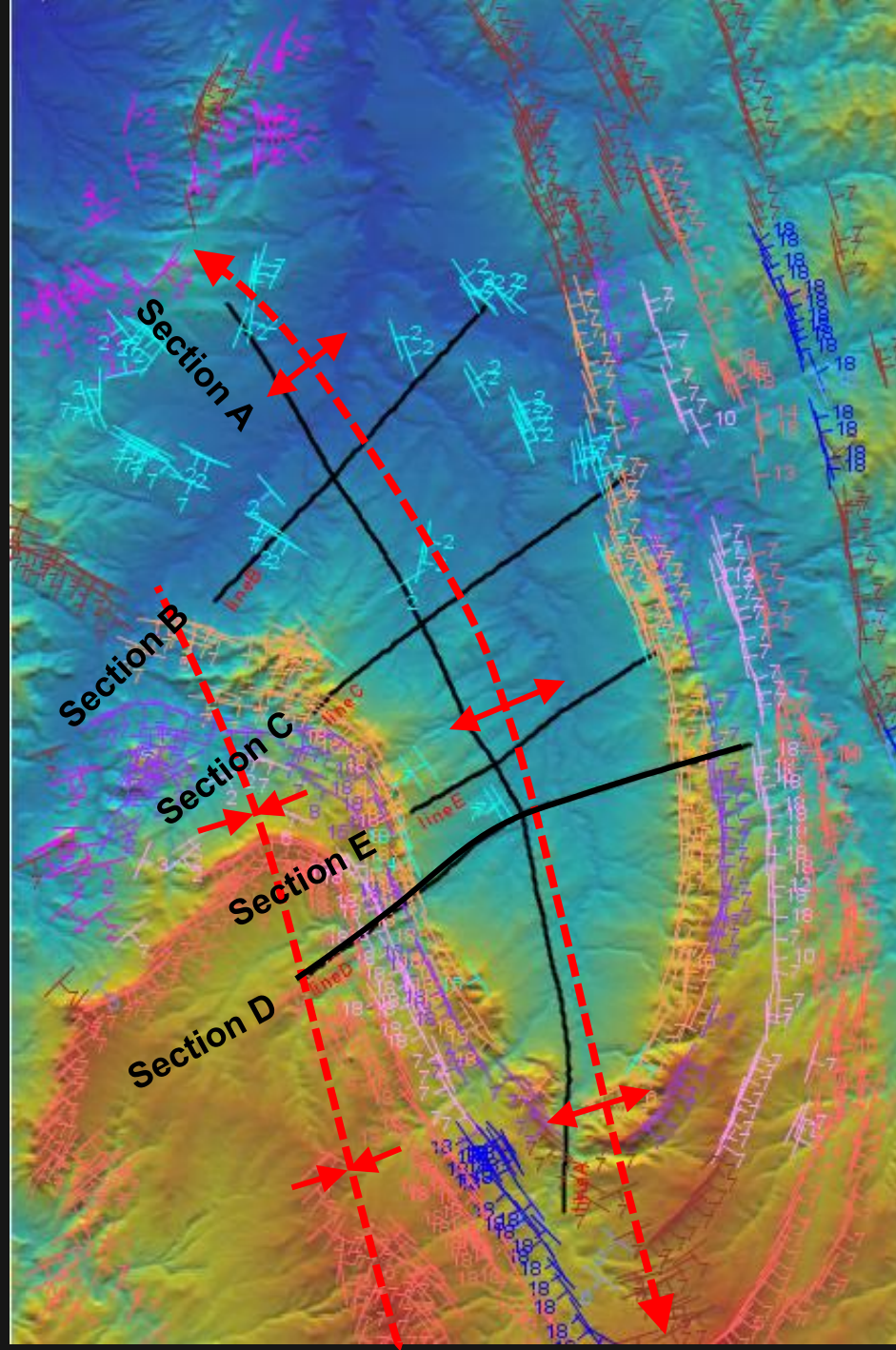
- Basement-cored, doubly plunging W-SW verging anticline
- E-NE dipping basement –involved blind thrust
- Four-way closure HC trap



Best Fit Plane (Rectangle)
Dip: 3.1
Dip Azimuth: 145.73
Best Fit Fold Axis (Triangle)
Trend: 154.65
Plunge: 3.06

Sample Size N: 857
Normalized Eigenvalues S1, S2, S3: 0.973, 0.025, 0.002
Shape Parameter K: 1.47
(girdle K<1; cluster K>1)
Strength Parameter C: 6.14
(weak C<3; strong C>3)
Uniformity Statistic Su: 3942.1
(deviation from uniformity: 95% Su>11.07; 99% Su>15.09)
[Refer to Help for more details.]

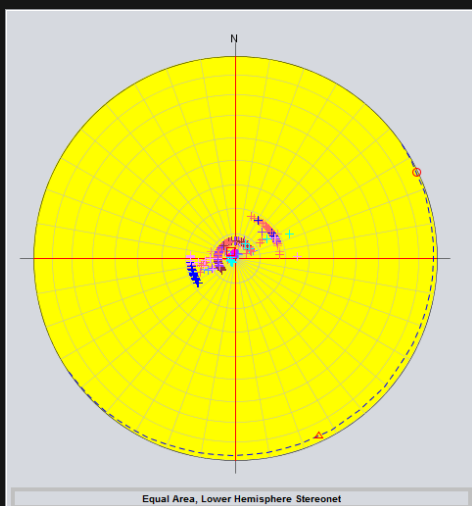
Eigenvector	Trend	Plunge	Eigenvalue
1 (Rectangle)	325.73	86.9	0.973
2 (Circle)	64.62	0.48	0.025
3 (Triangle)	154.65	3.06	0.002



Teapot Dome, WY

- Basement-cored, doubly plunging W-SW verging anticline
- E-NE dipping basement –involved blind thrust
- Four-way closure HC trap

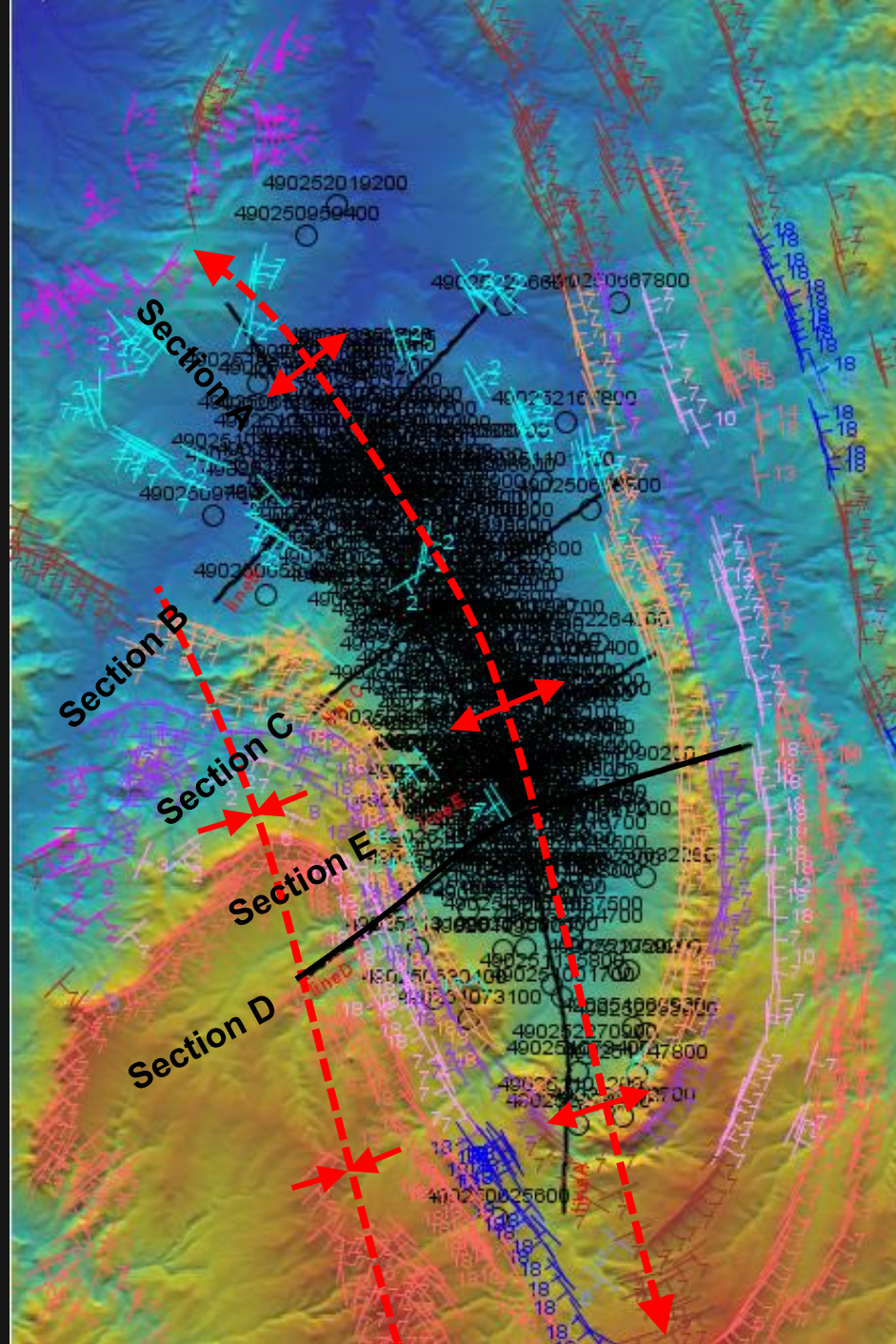
Wells mainly in the fold hinge/crest!



Best Fit Plane (Rectangle)
Dip: 3.1
Dip Azimuth: 145.73
Best Fit Fold Axis (Triangle)
Trend: 154.65
Plunge: 3.06

Sample Size N: 857
Normalized Eigenvalues S1, S2, S3: 0.973, 0.025, 0.002
Shape Parameter K: 1.47
(girdle K<1; cluster K>1)
Strength Parameter C: 6.14
(weak C<3; strong C>3)
Uniformity Statistic Su: 3942.1
(deviation from uniformity: 95% Su>11.07; 99% Su>15.09)
[Refer to Help for more details.]

Eigenvector	Trend	Plunge	Eigenvalue
1 (Rectangle)	325.73	86.9	0.973
2 (Circle)	64.62	0.48	0.025
3 (Triangle)	154.65	3.06	0.002



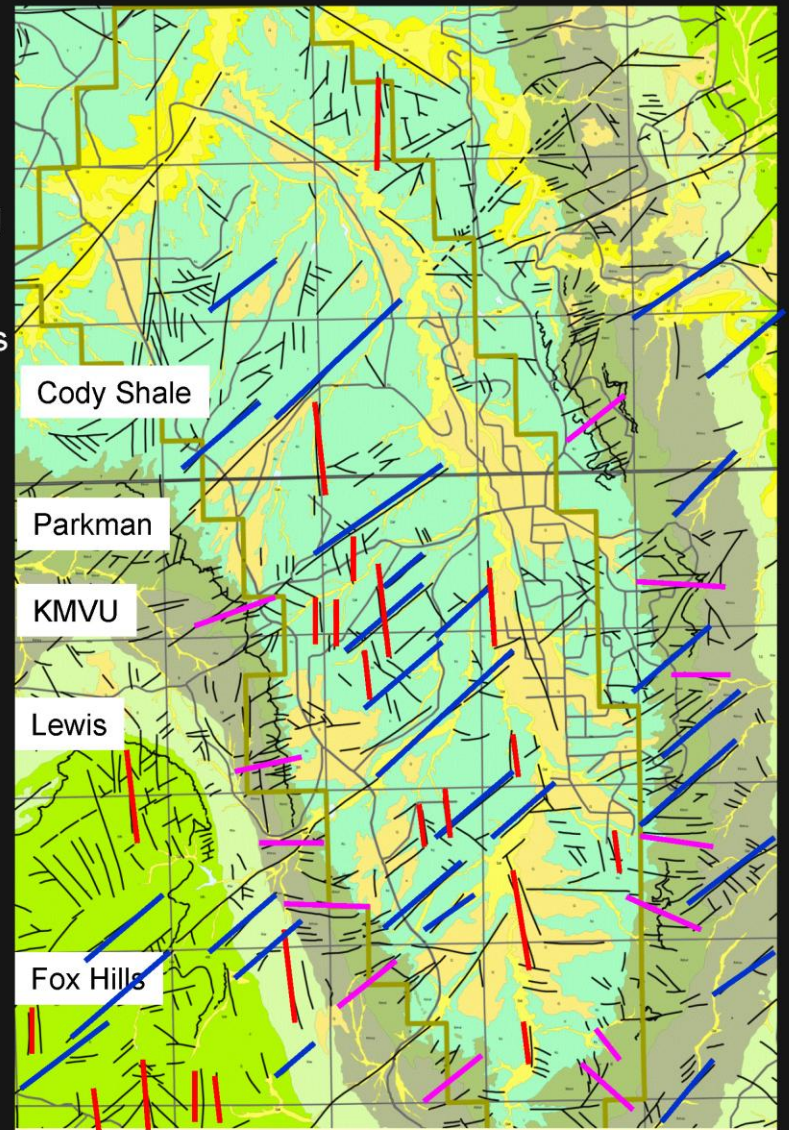
Natrona County, Wyoming
T 38 & 39 N R 78 W

	CENTER				
Period	Formation	Lithology	Thickness	Depth (ft)	Productive
Quaternary	Alluvium		0-50		
	Fox Hills Sandstone		100		
	Lewis Shale		600		
	Mesaverde Group	Pegtop Ss Pumpkin Buttes shale Parkman Ss	50 325 470		
			480		
		Sussex Ss	195 30	195	
	Steele Shale		290		
		Shannon Ss	120	515 635	■
			1355		■
	Niobrara Shale		450	1990	■
	Carlisle Shale		240	2440	
		1st Wall Creek	160	2680	
			245	2840	
	Frontier	2nd Wall Creek	65	3085	■
			175	3150	
		3rd Wall Creek	5	3325	■
			265	3330	
	Mowry Shale		230	3595	
		Muddy Sandstone	15	3825	
		Thermopolis Shale	135	3840	
		Dakota	85	3975	
			10	4065	■
		Lakota	270	4070	
	Morrison		270		
Jurassic	Sundance	Upper	95	4340	
		Lower	150	4435	
		Crow Mountain	80		
		Alcova LS	20	4665	
	Chugwater Group	Red Peak	520	4685	
Permian	Goose Egg		320	5205	
	Tensleep		320	5525	■
	Amsden		160	5845	
Mississippian	Madison		300	6005	
Devonian through Cambrian	Undifferentiated		780	6305	
Pre-Cambrian	Granite		7085		

Over 22 MM barrels
of oil since 1976

Several oil-producing formations

- Tensleep Ss
- 2nd Wall Creek Ss
- Shannon Ss
- Muddy Ss
- Dakota Ss



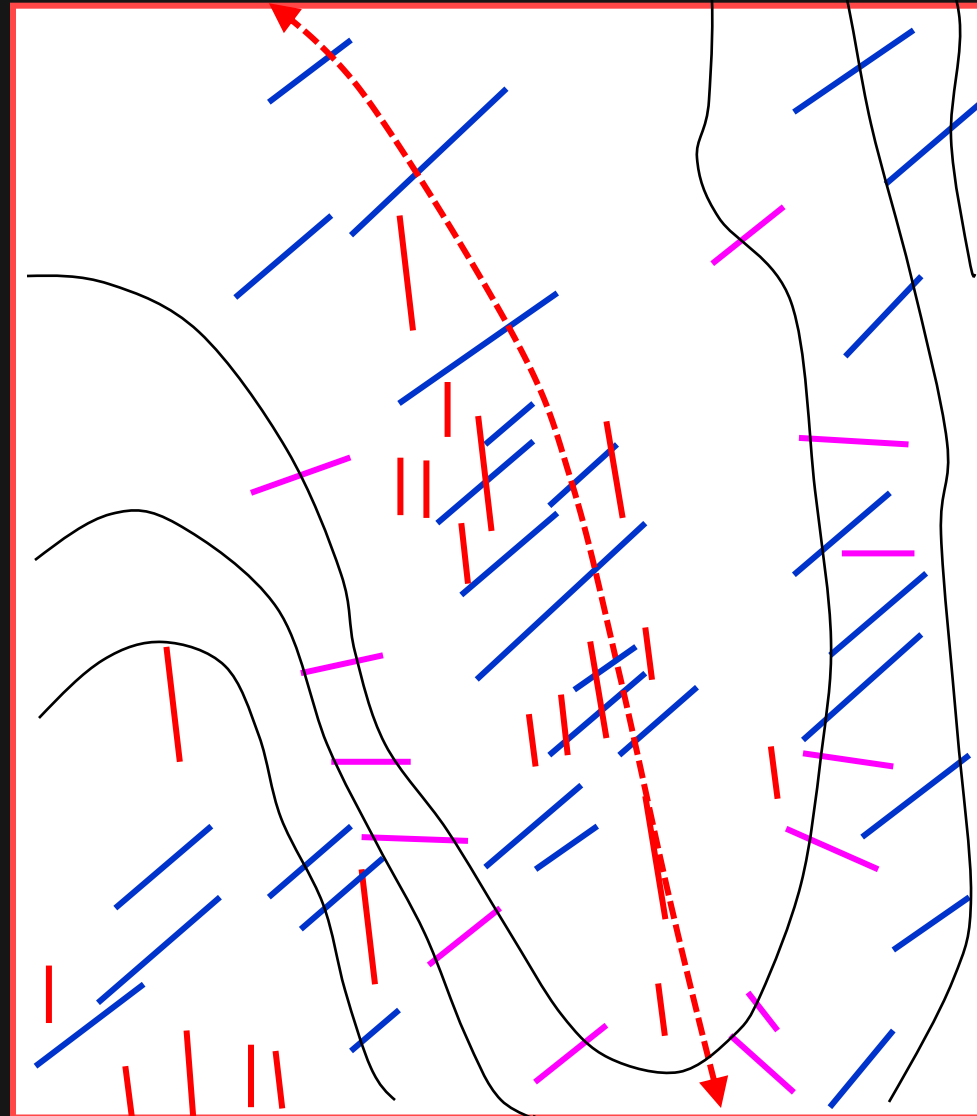
Presenter's notes: Geologic map with fractures.

Three prominent open fracture systems:

1. hinge-oblique (NW)
2. hinge-parallel (NNE)
3. hinge-perpendicular (radial)

Maximum permeability

- mainly parallel to fold hinge
- locally also perpendicular to fold hinge where NE-striking cross faults
- Intersections of hinge-parallel and hinge-perpendicular faults and fractures increase interconnectivity and enhance permeability



Type I fracture set

- Tensional fractures perpendicular to fold axis
- Rotates around plunge of fold
- Mainly along fold limbs

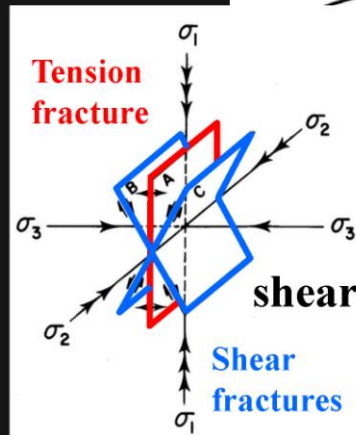
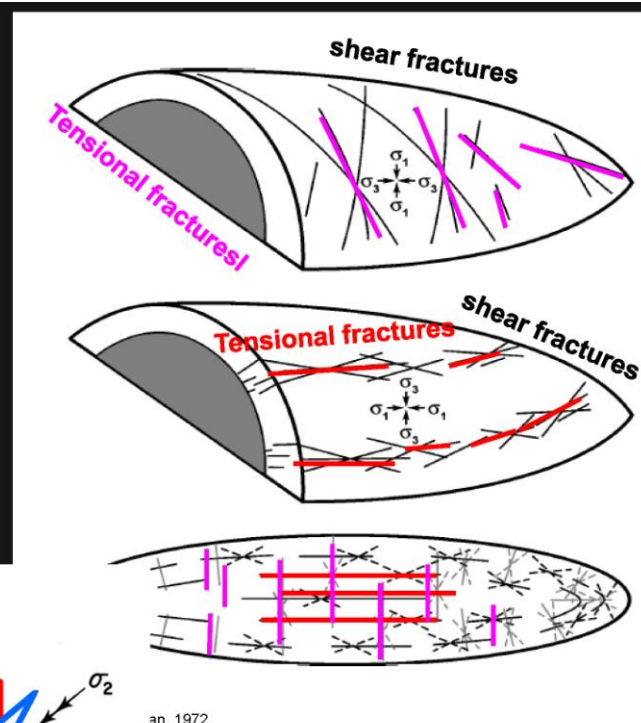
Type II fracture set

- Tensional fractures parallel to fold axis
- Mainly along hinge

Third oblique fracture set

- Dominant tensional fractures oblique to fold axis
- May be pre-folding

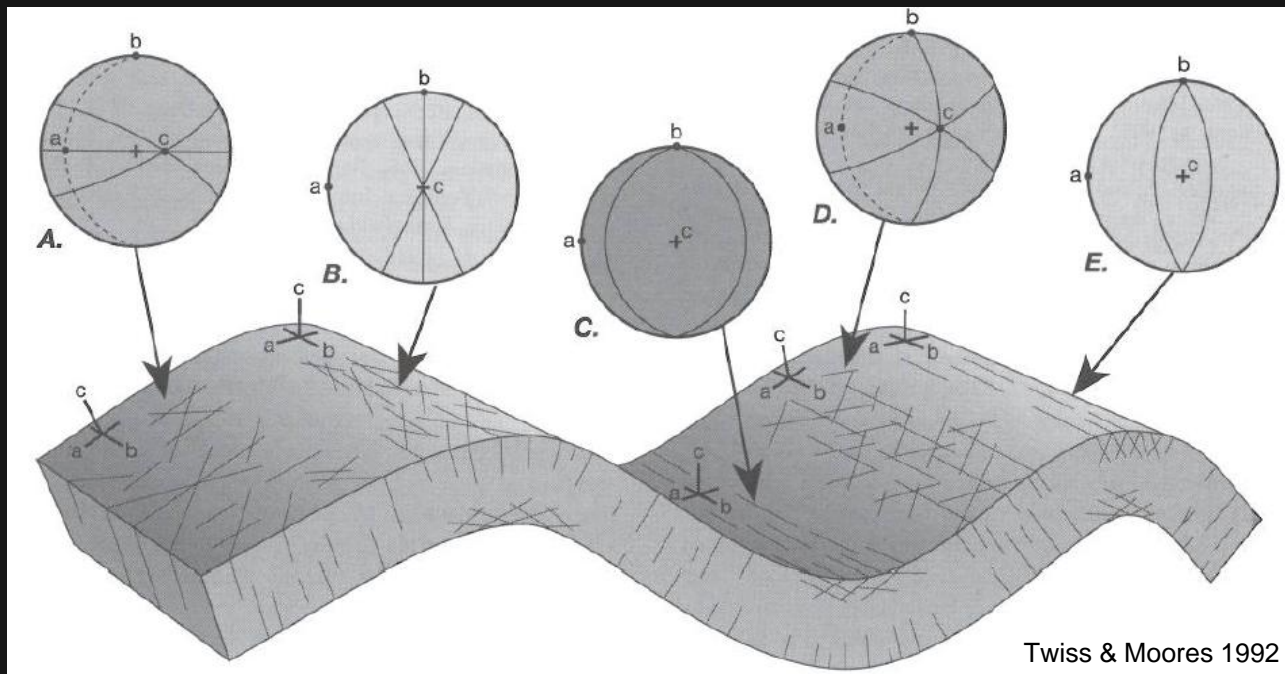
© 2014 HALLIBURTON. ALL RIGHTS RESERVED.



Presenter's notes: A genetic classification divides fractures into Type I and Type II (Stearns, 1968). Type I fractures are composed of a tensional set oriented perpendicular to the fold axis with an associated conjugate shear set whose acute bisector coincides with the orientation of tensional fractures. Type II fractures are composed of an extensional set oriented parallel to the fold axis with an associated conjugate shear set whose acute bisector coincides with the orientation of extensional fractures. Consequently, open fractures are classified as tensional, extensional, or shear sets with orientation perpendicular, parallel, or oblique to the structural axis.

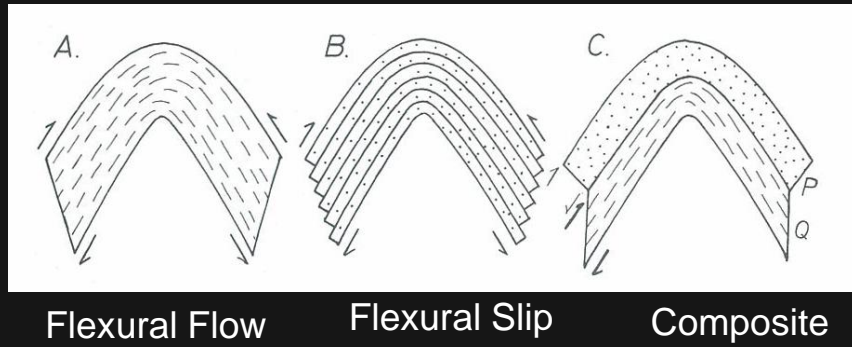
Fold 1B-types and their fracture patterns

- The orientation and localization of the reservoir fracture population depends on the dominant folding mechanism.
- Fractures concentrate at certain domains of the fold morphology.

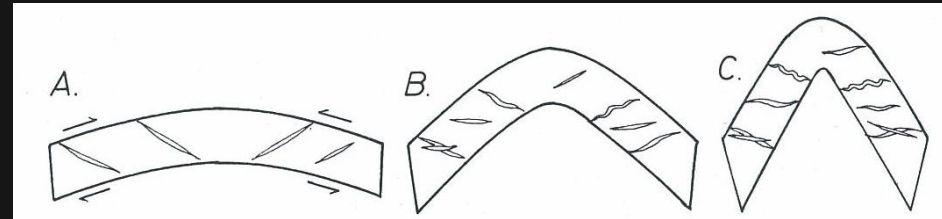


Typical fracture patterns due to folding (concentric-parallel folds)

Fold 1B-types and their fracture patterns

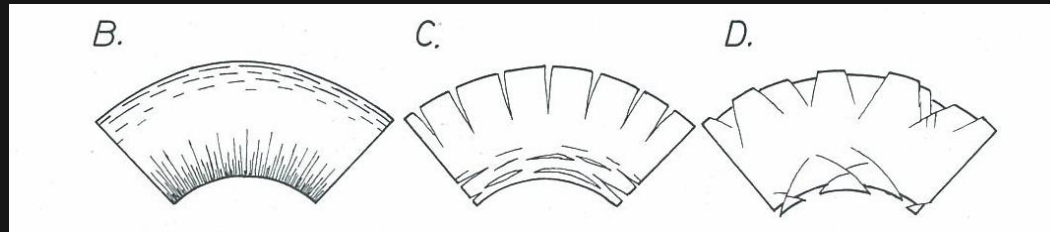


Flexural flow + parallel folds

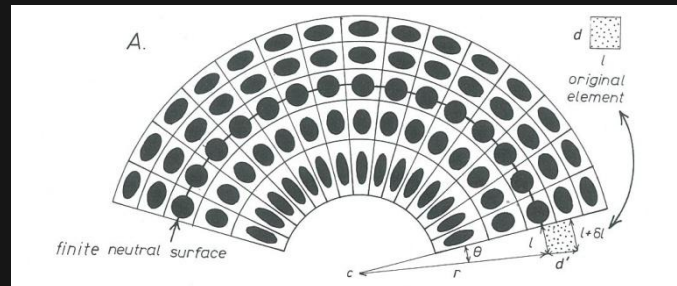
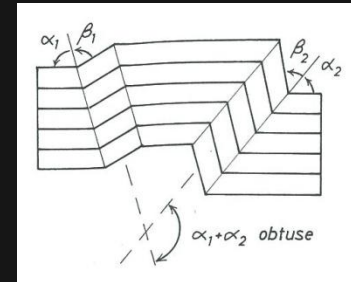


Progressive development of shear fractures in flexural slip folds

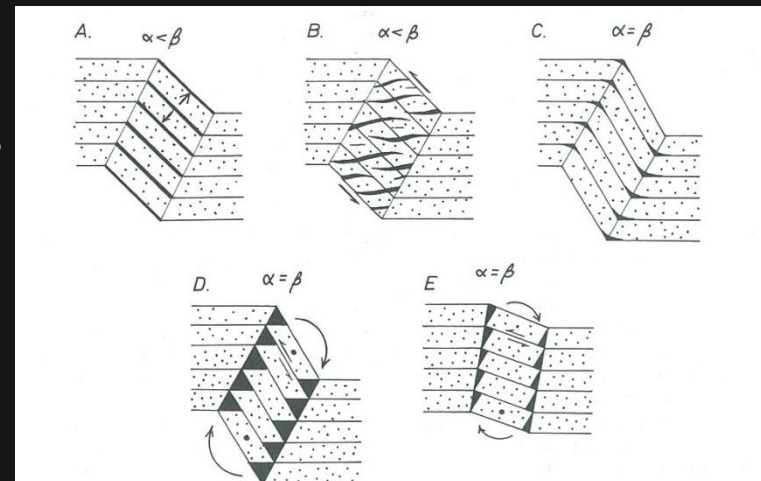
Tangential Longitudinal Strain



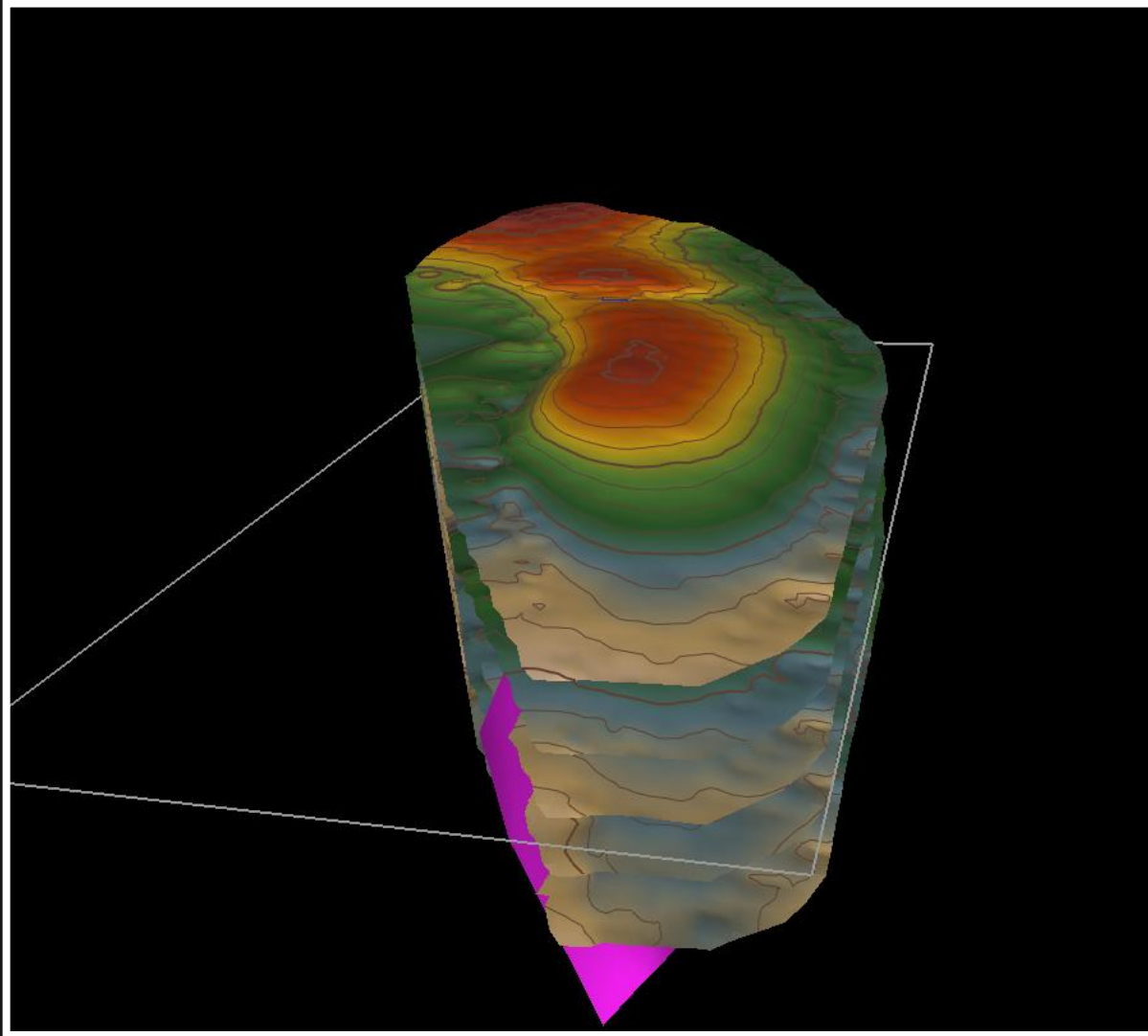
Kink Fold



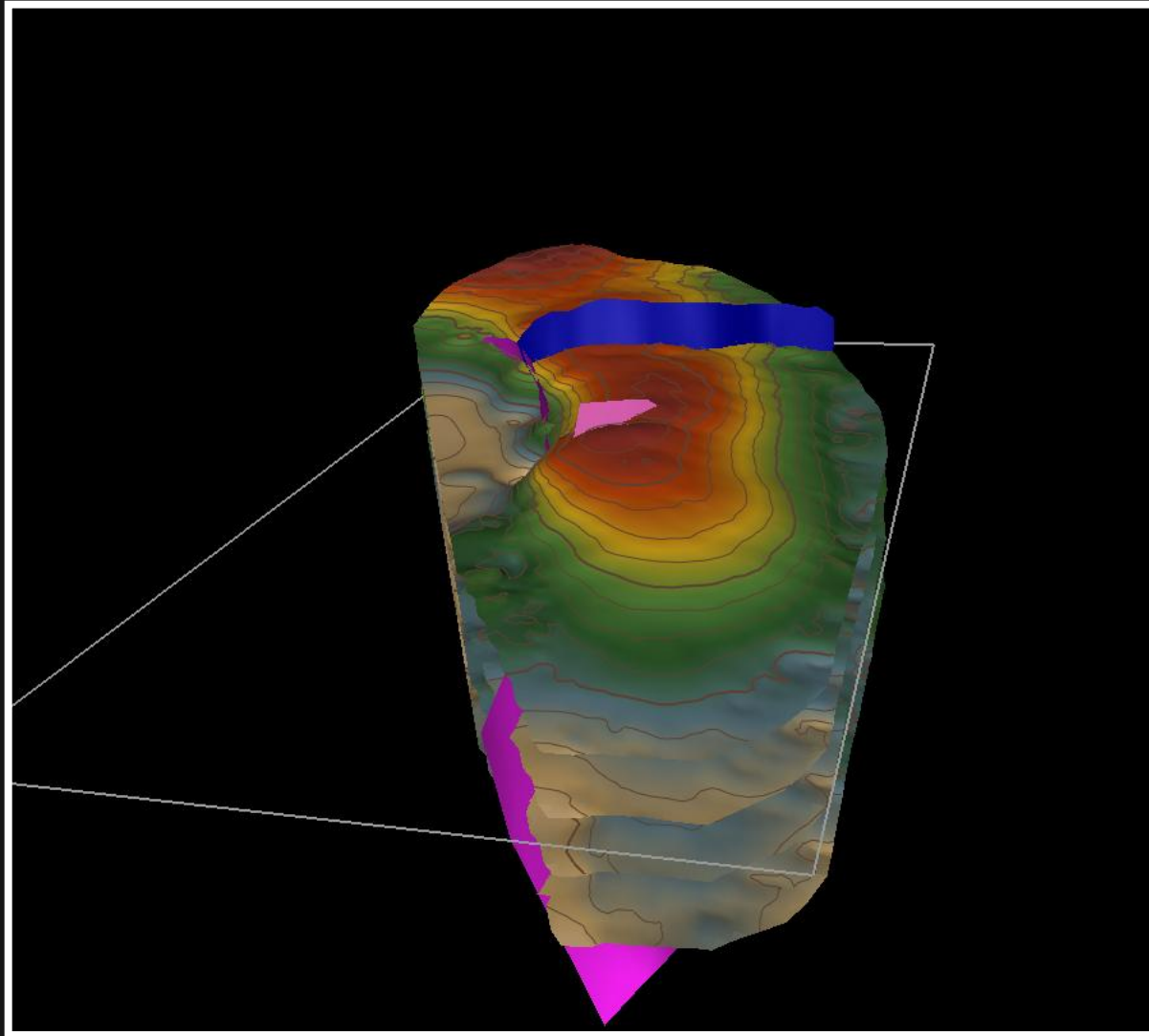
Parallel (Bend) Folds



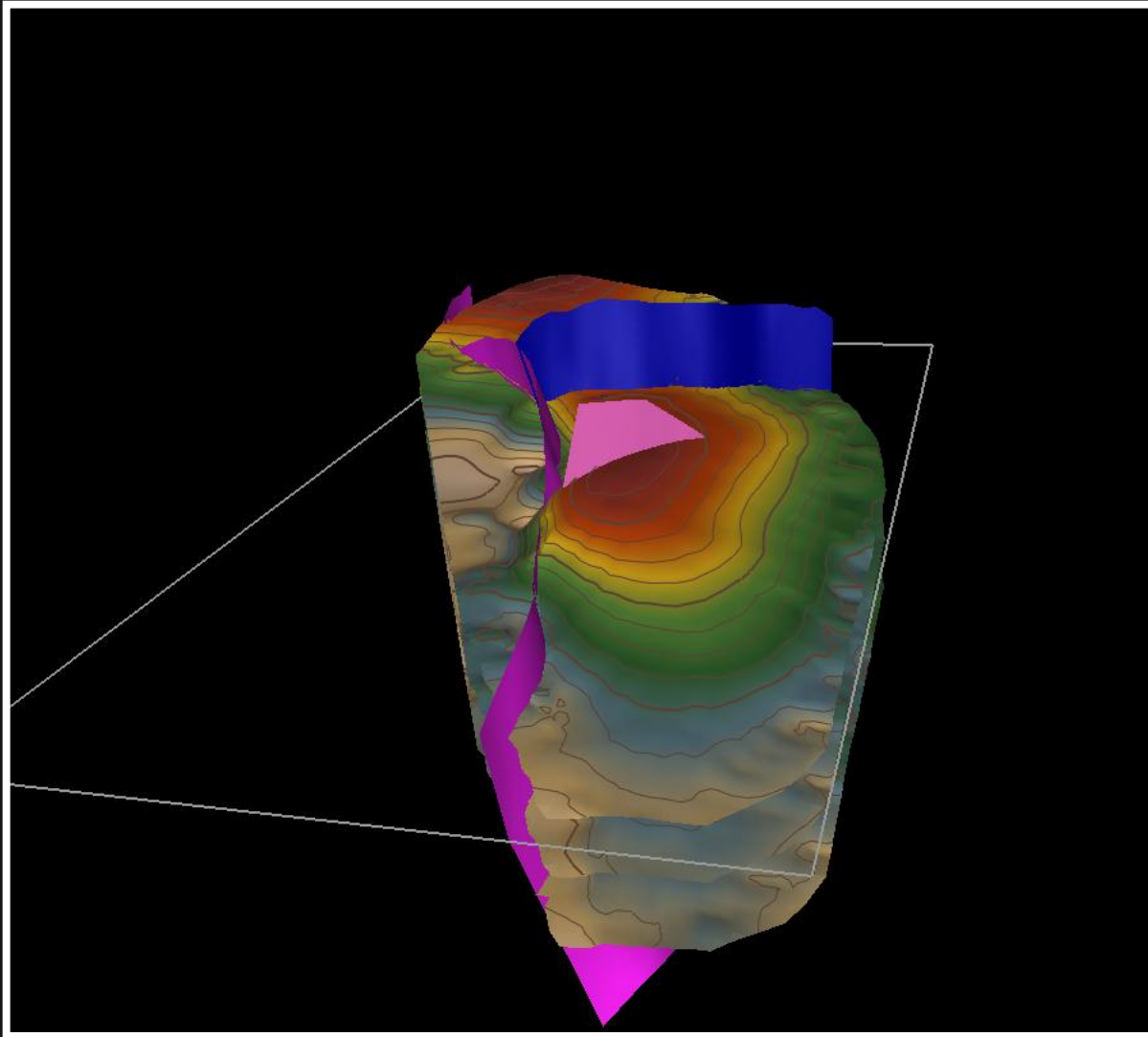
Teapot Dome 3D structure



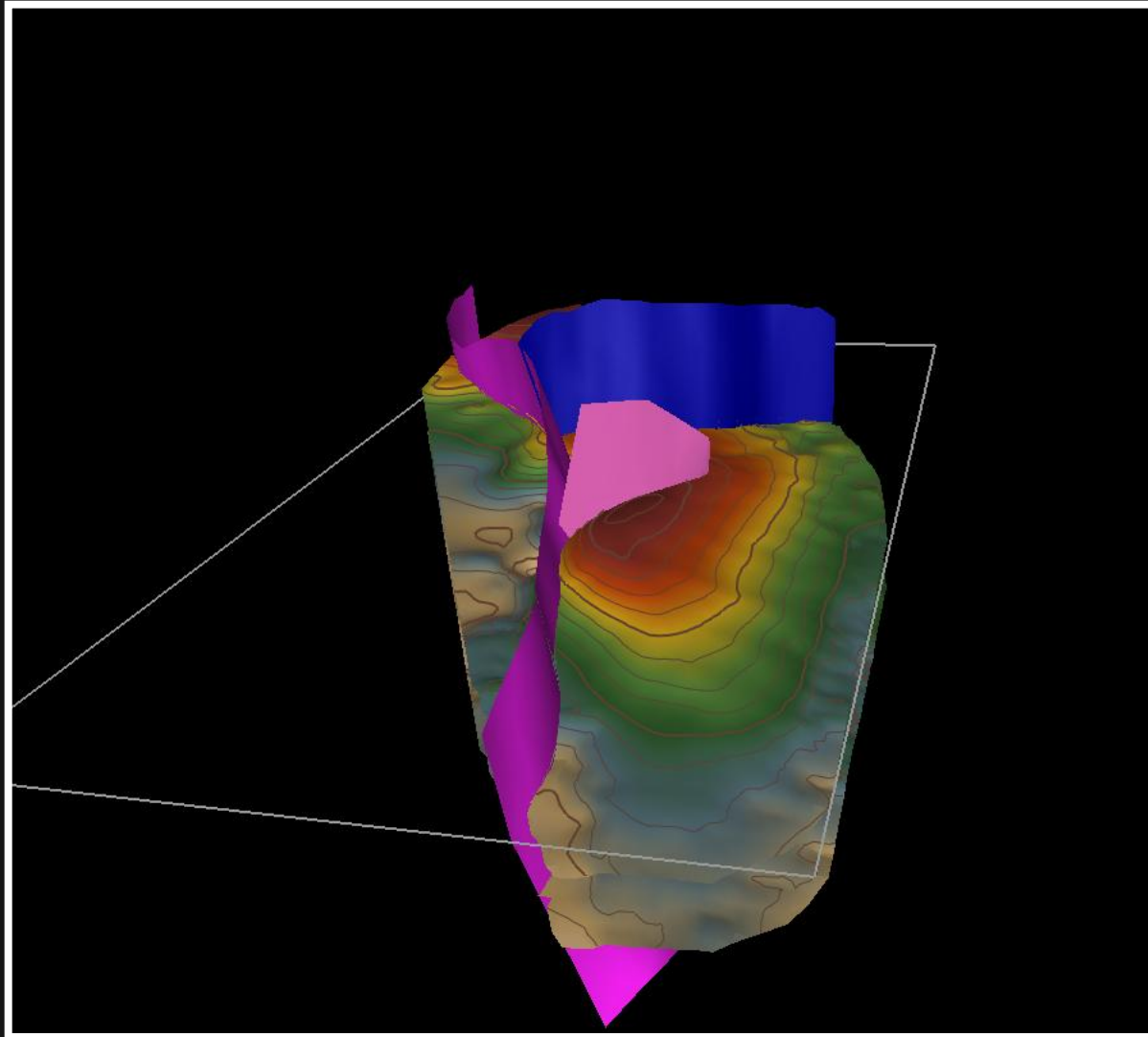
Teapot Dome 3D structure



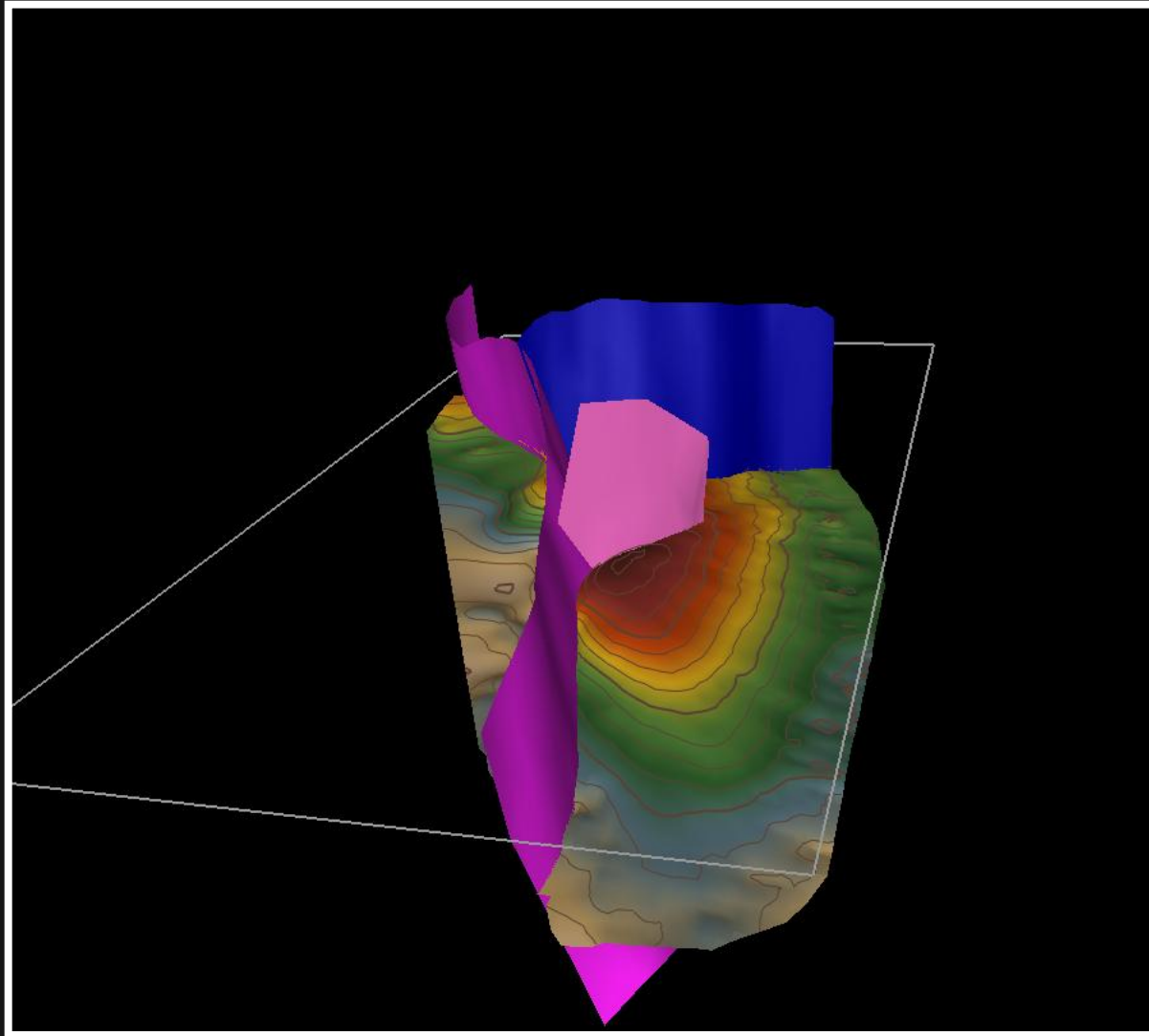
Teapot Dome 3D structure



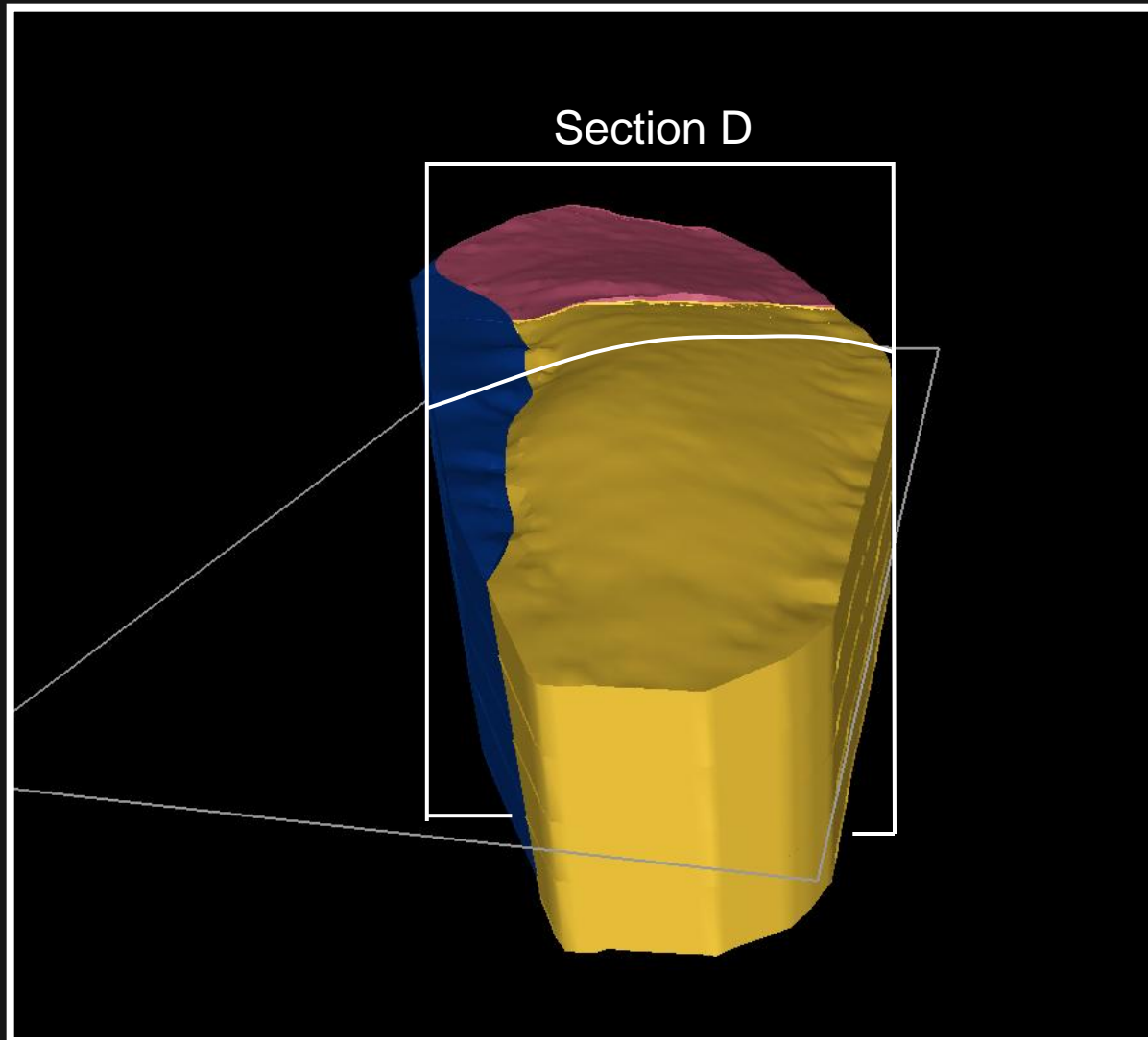
Teapot Dome 3D structure



Teapot Dome 3D structure



Teapot Dome 3D structure



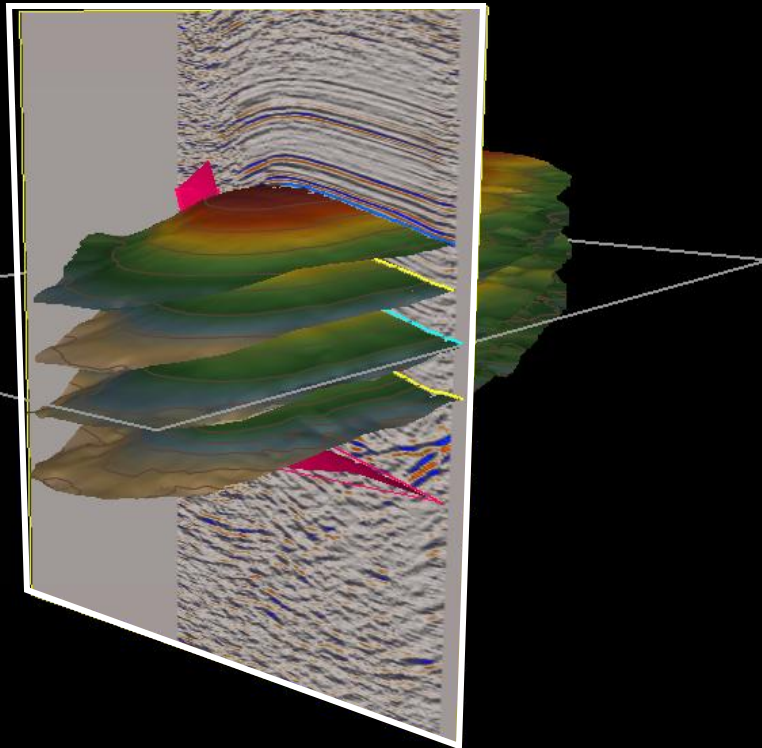
The role of the Teapot Dome fault

Fault location and trajectory critical for:

- structural analysis and 2D/3D modeling
- strain distribution modeling
- volume estimates
- controls of deformation on fracture permeability

Fault interpretations:

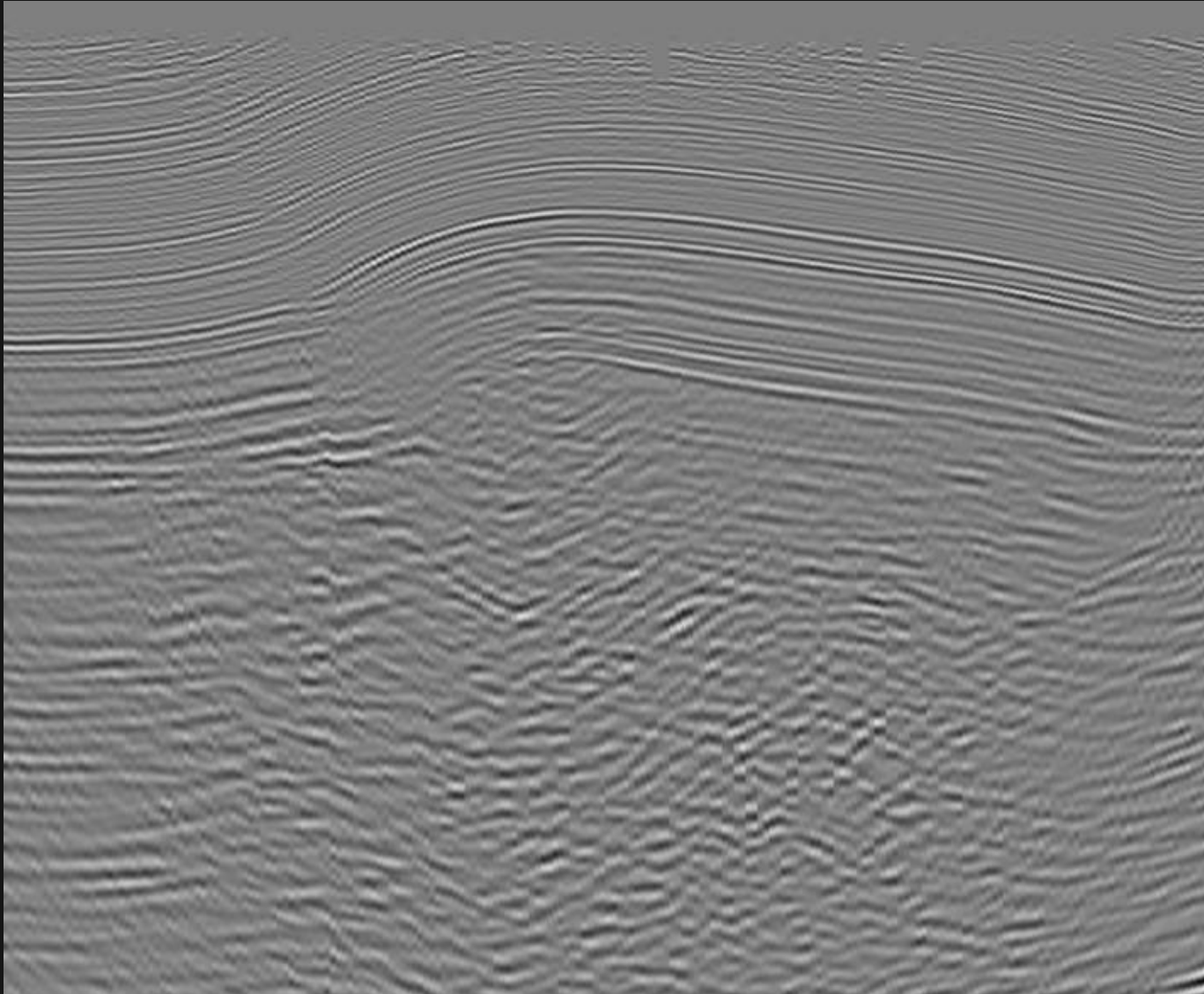
- Extensional normal fault
- Basement-involved blind thrust fault with unconstrained trajectory
- Thrust fault
- Fold bend fold



WSW

Section D

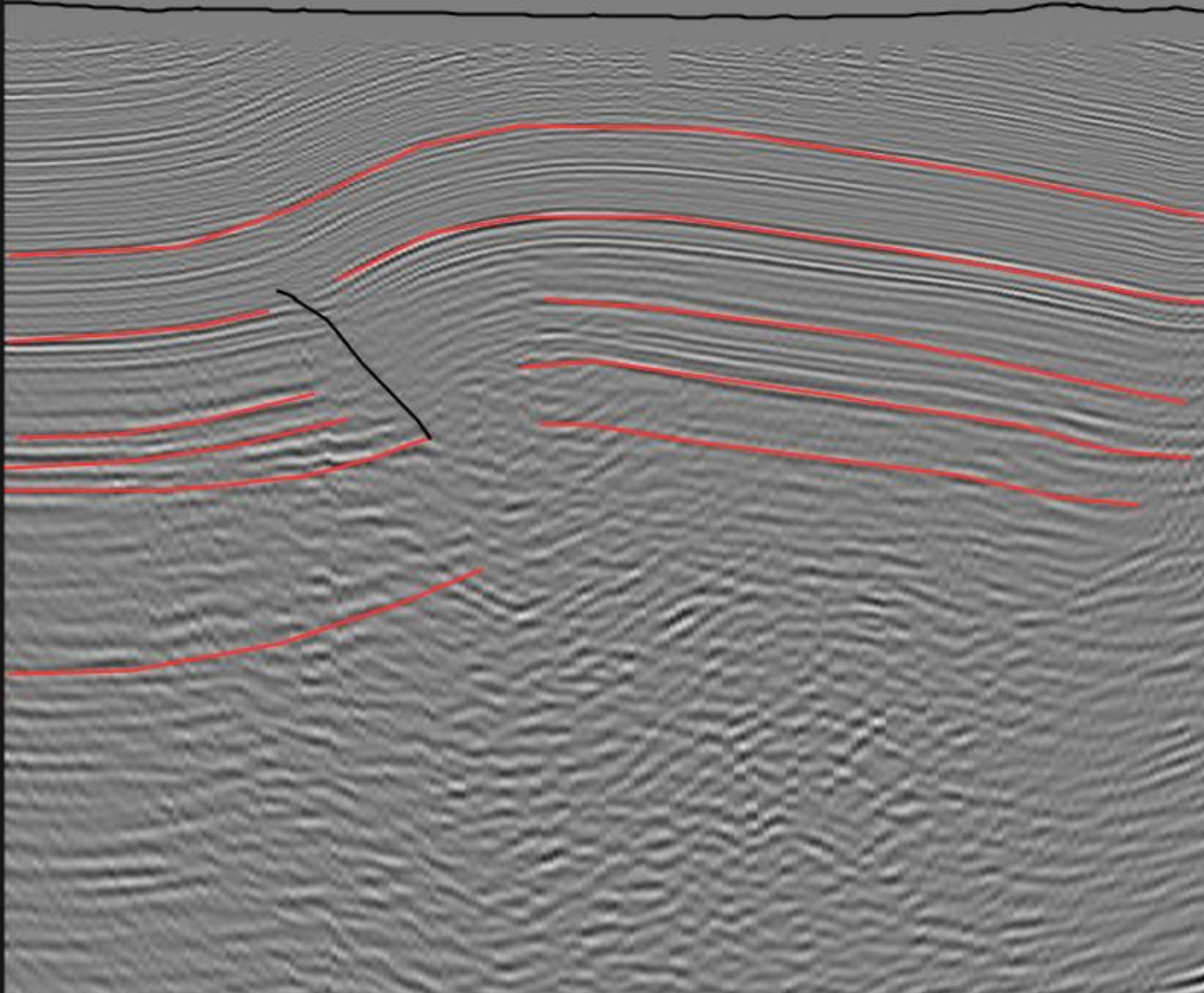
ENE



WSW

Section D

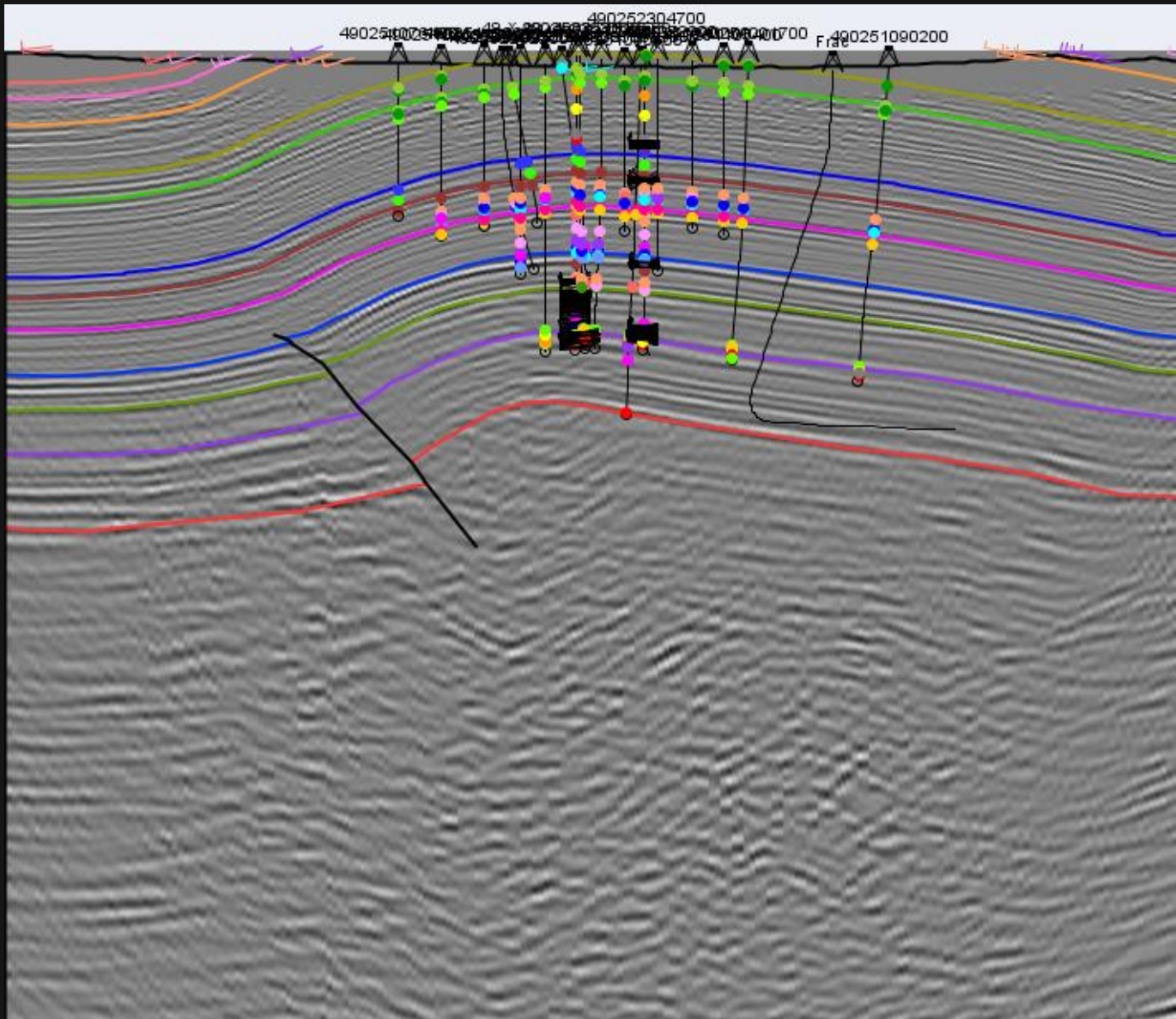
ENE

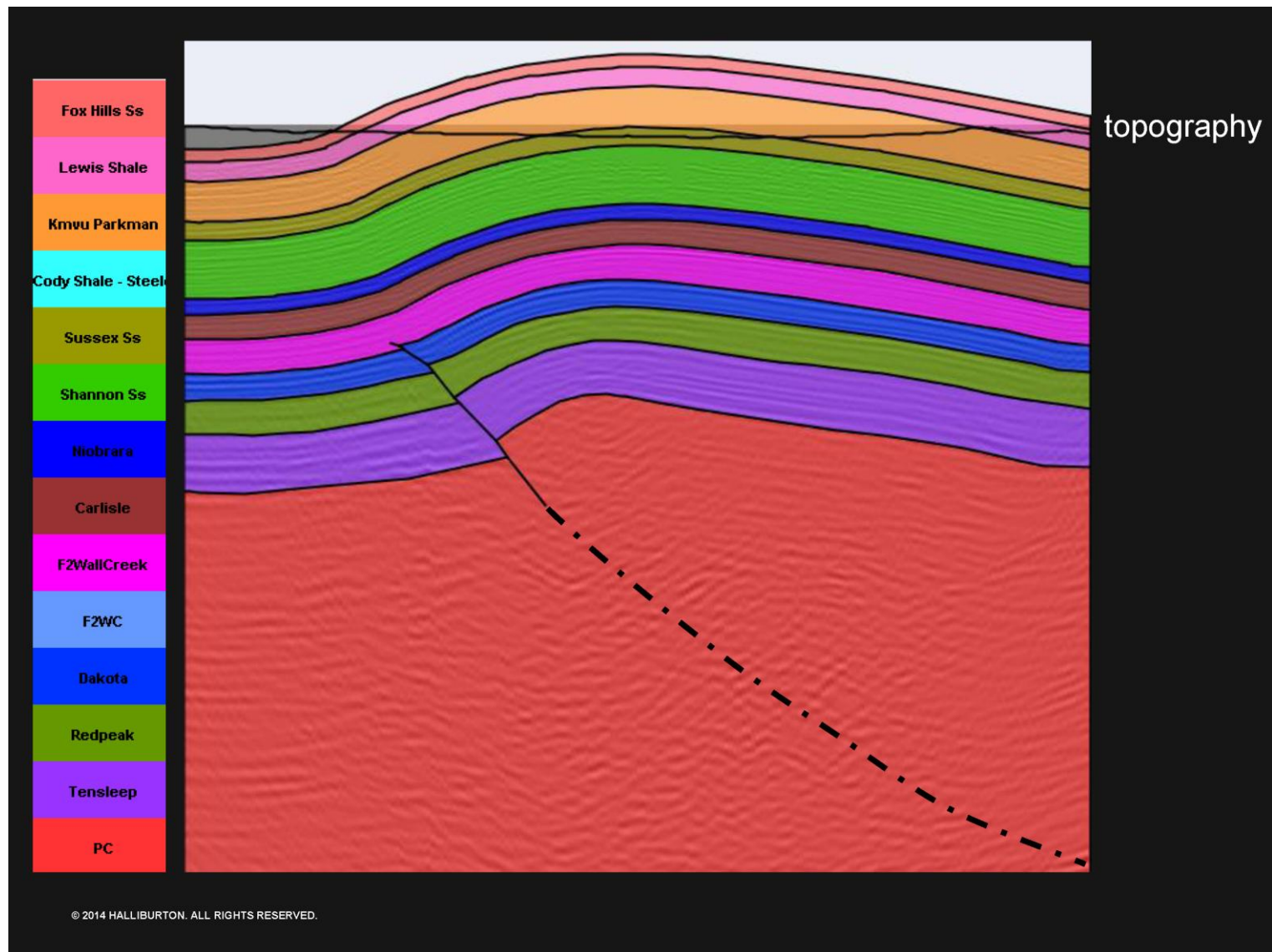


WSW

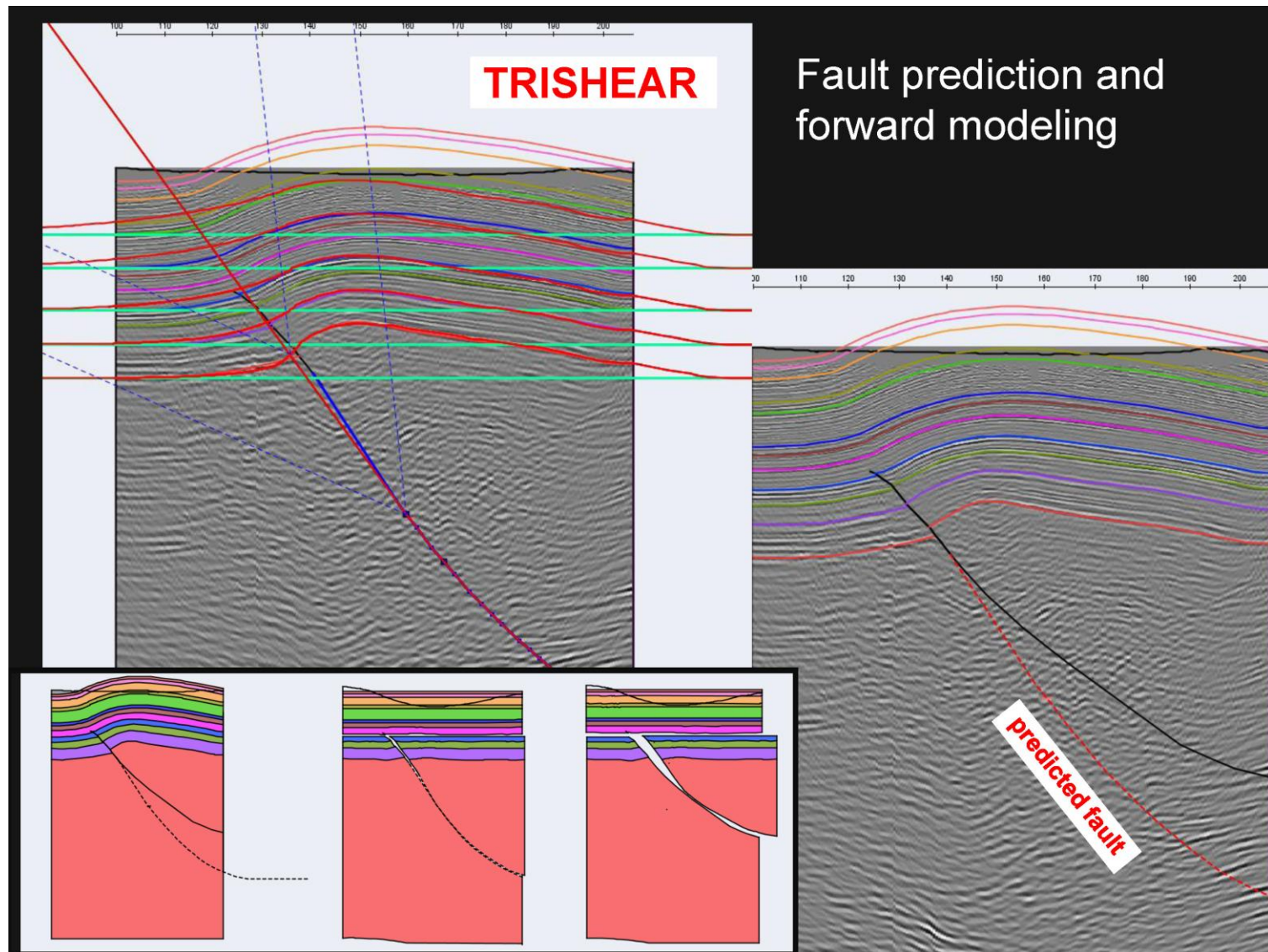
Section D

ENE



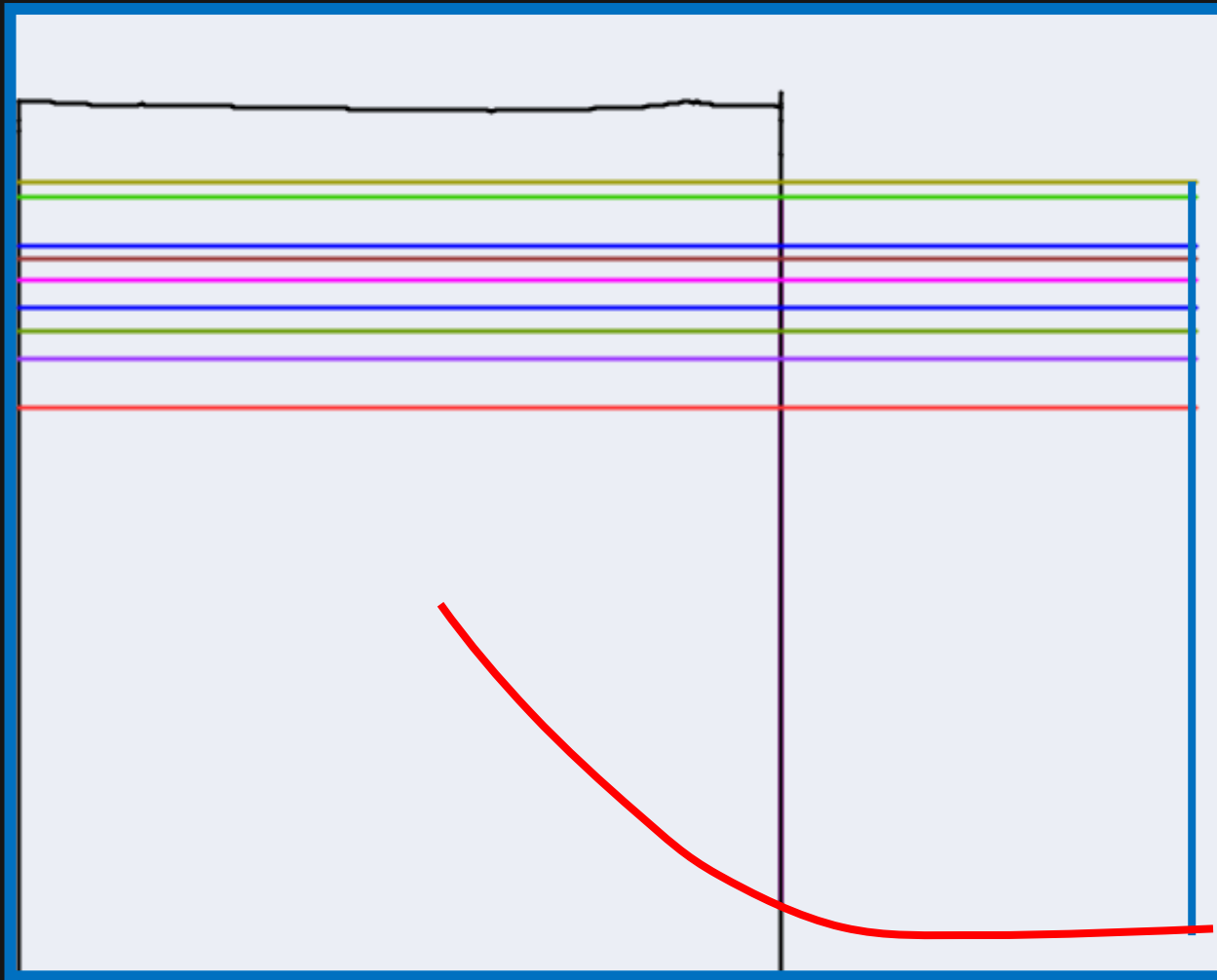


Presenter's notes: Original interpretation.

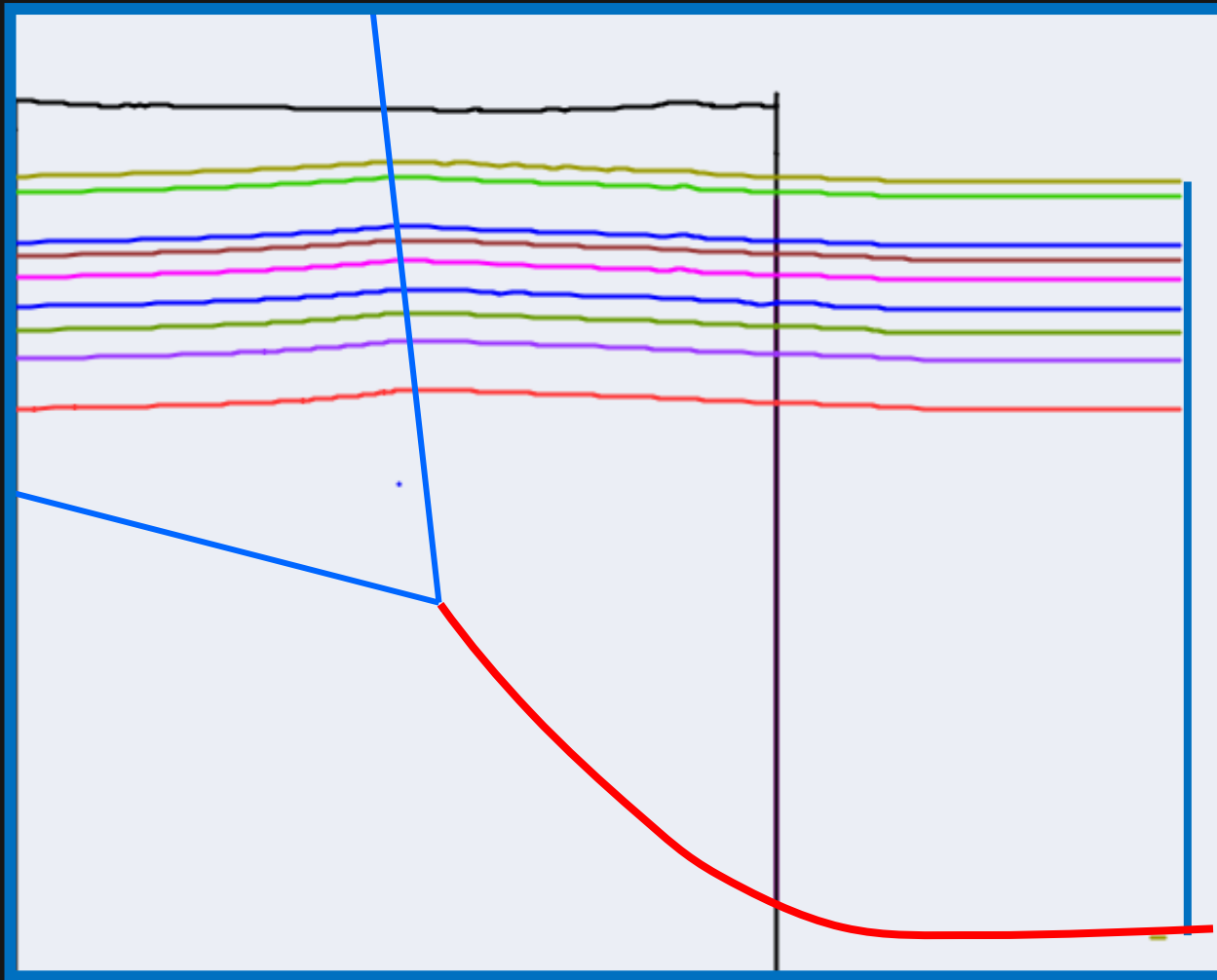


Presenter's notes: Predict fault trace based on hangingwall and footwall and cutoffs--steeper fault that probably soles out.

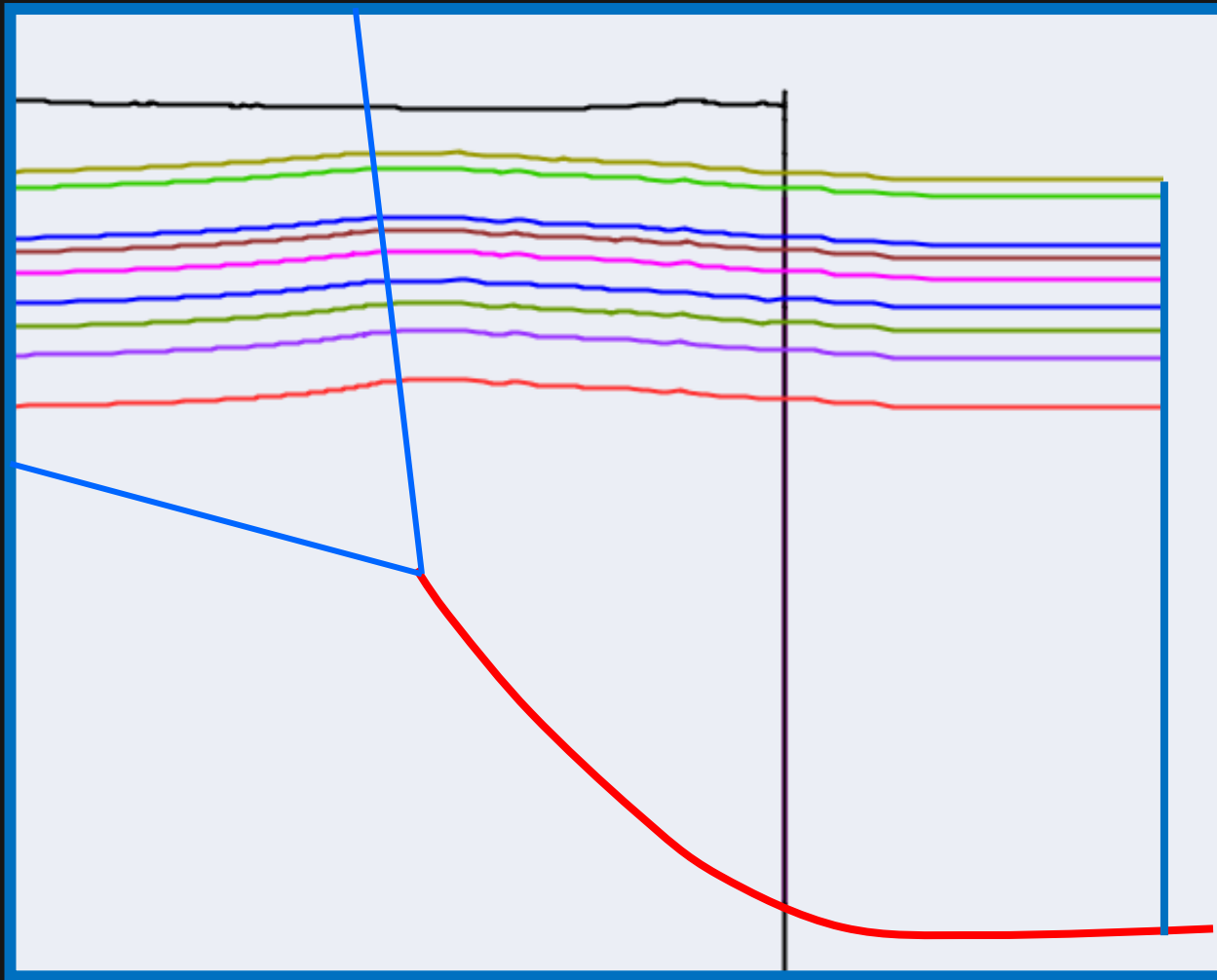
Forward modeling with trishear



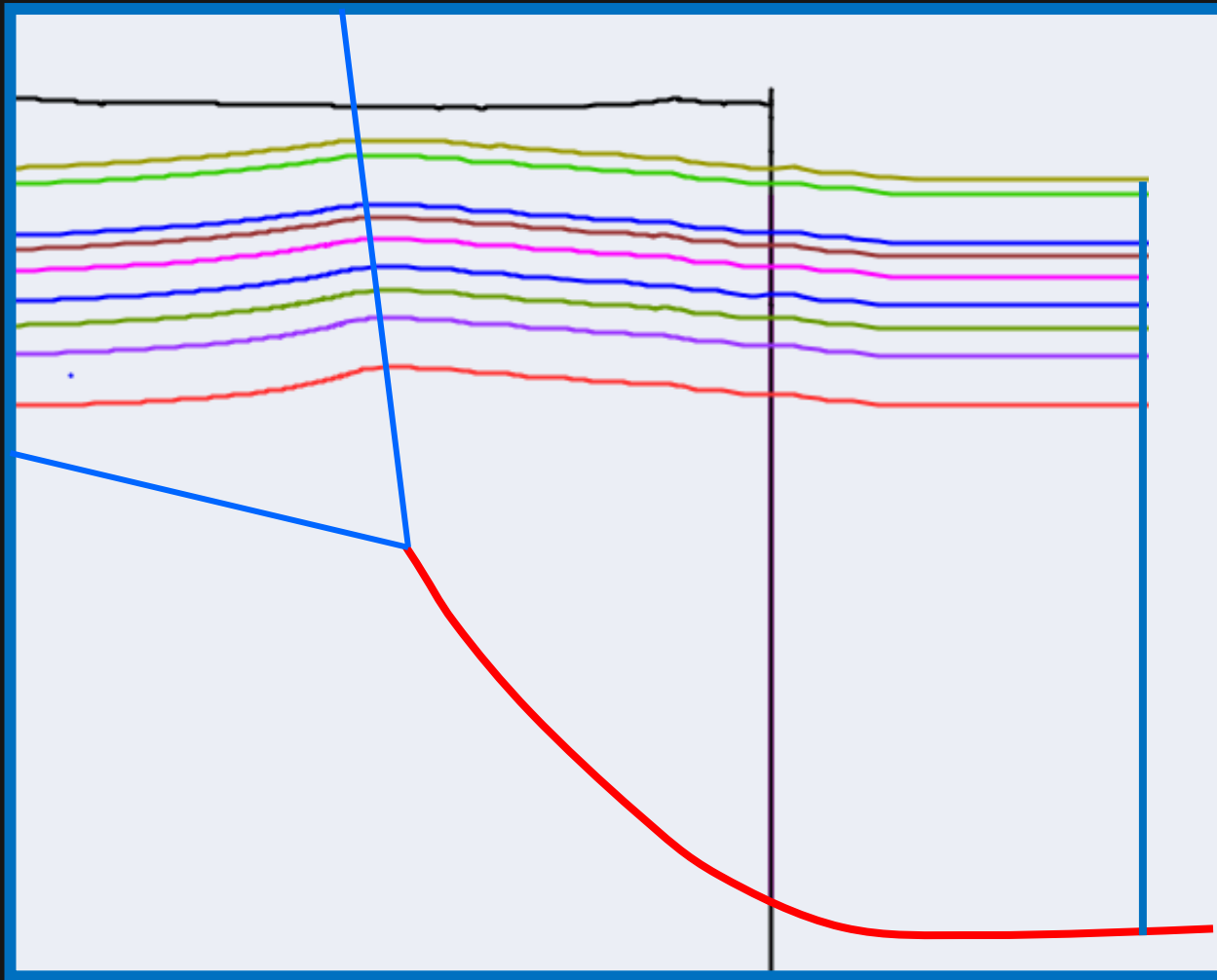
Forward modeling with trishear



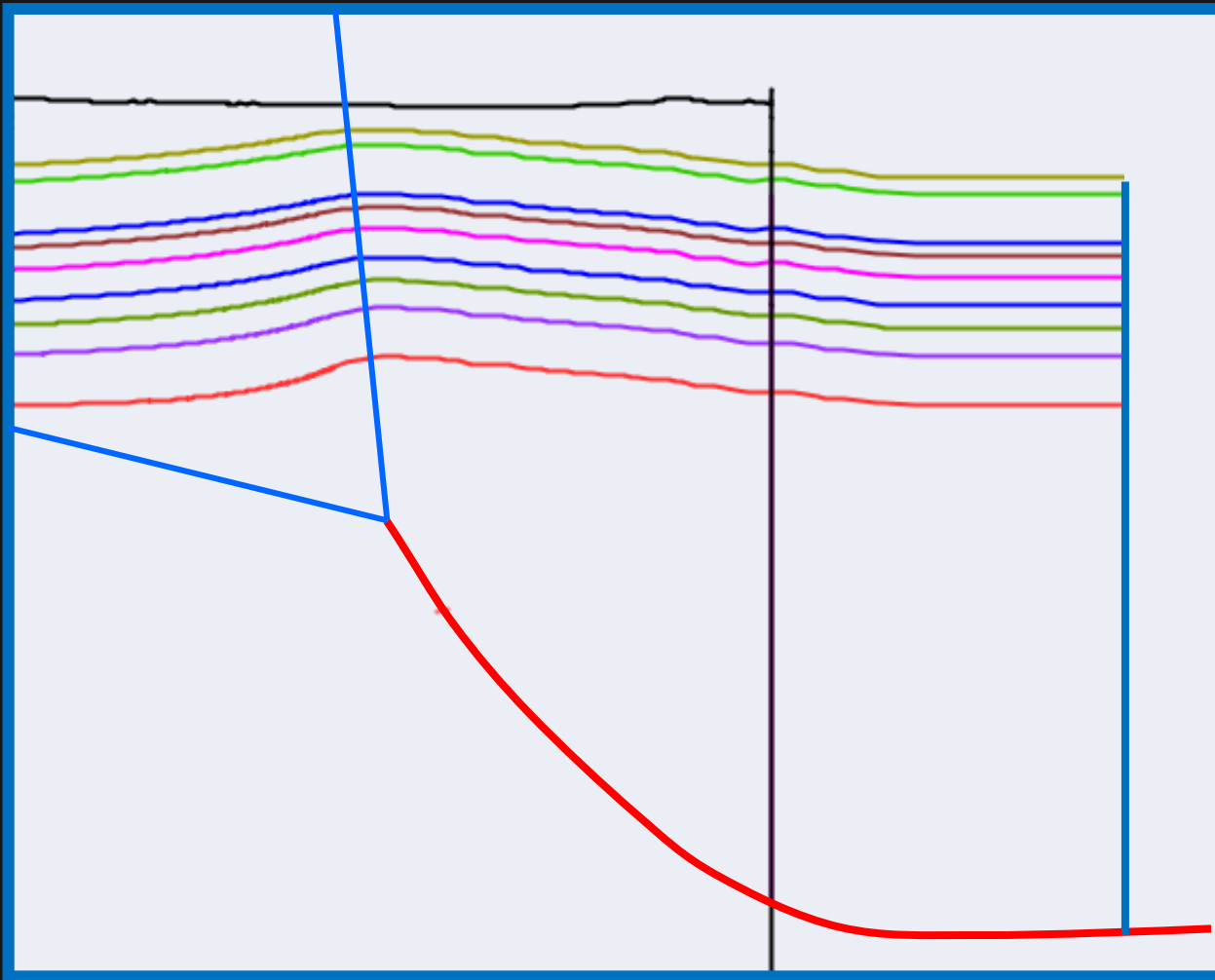
Forward modeling with trishear



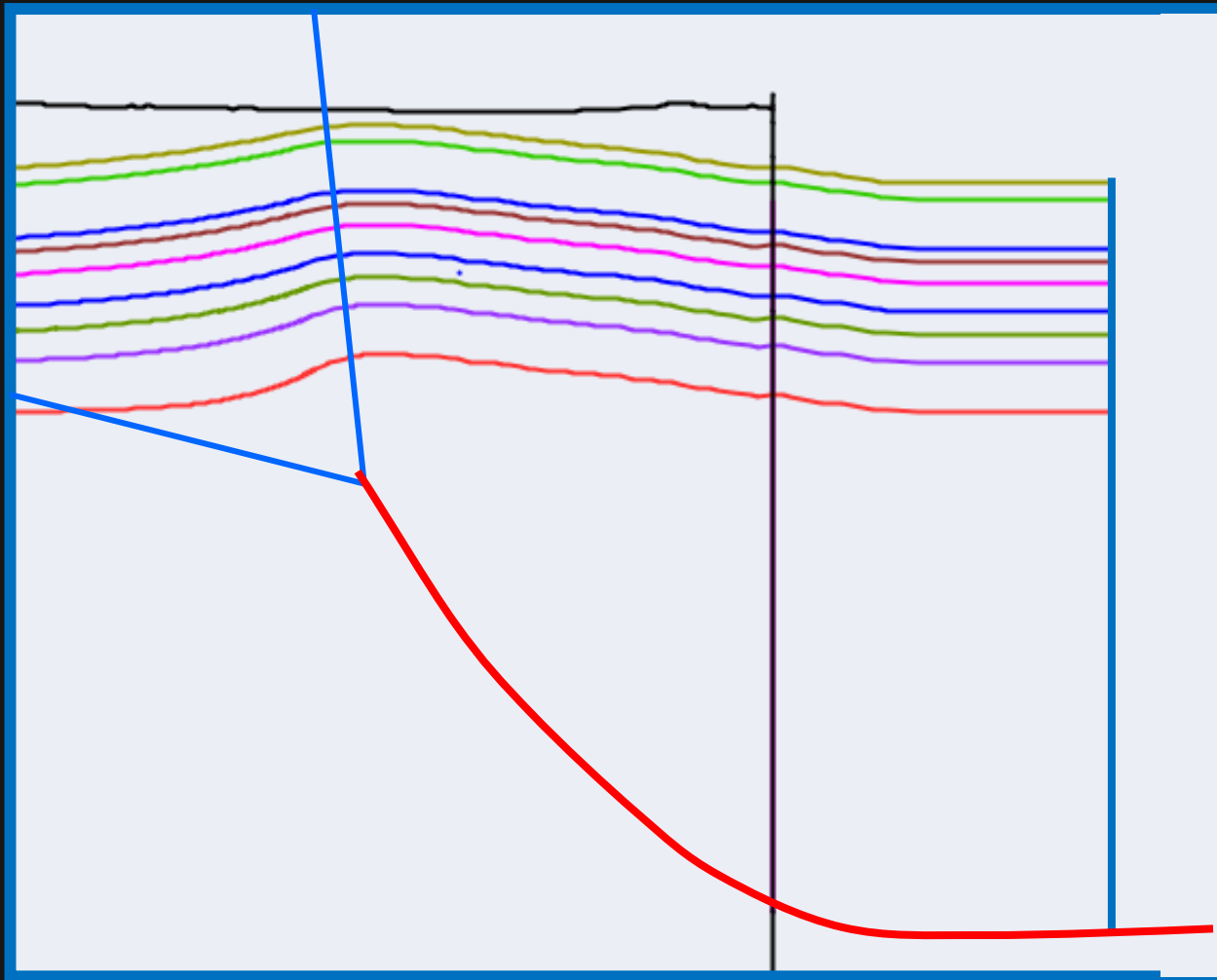
Forward modeling with trishear



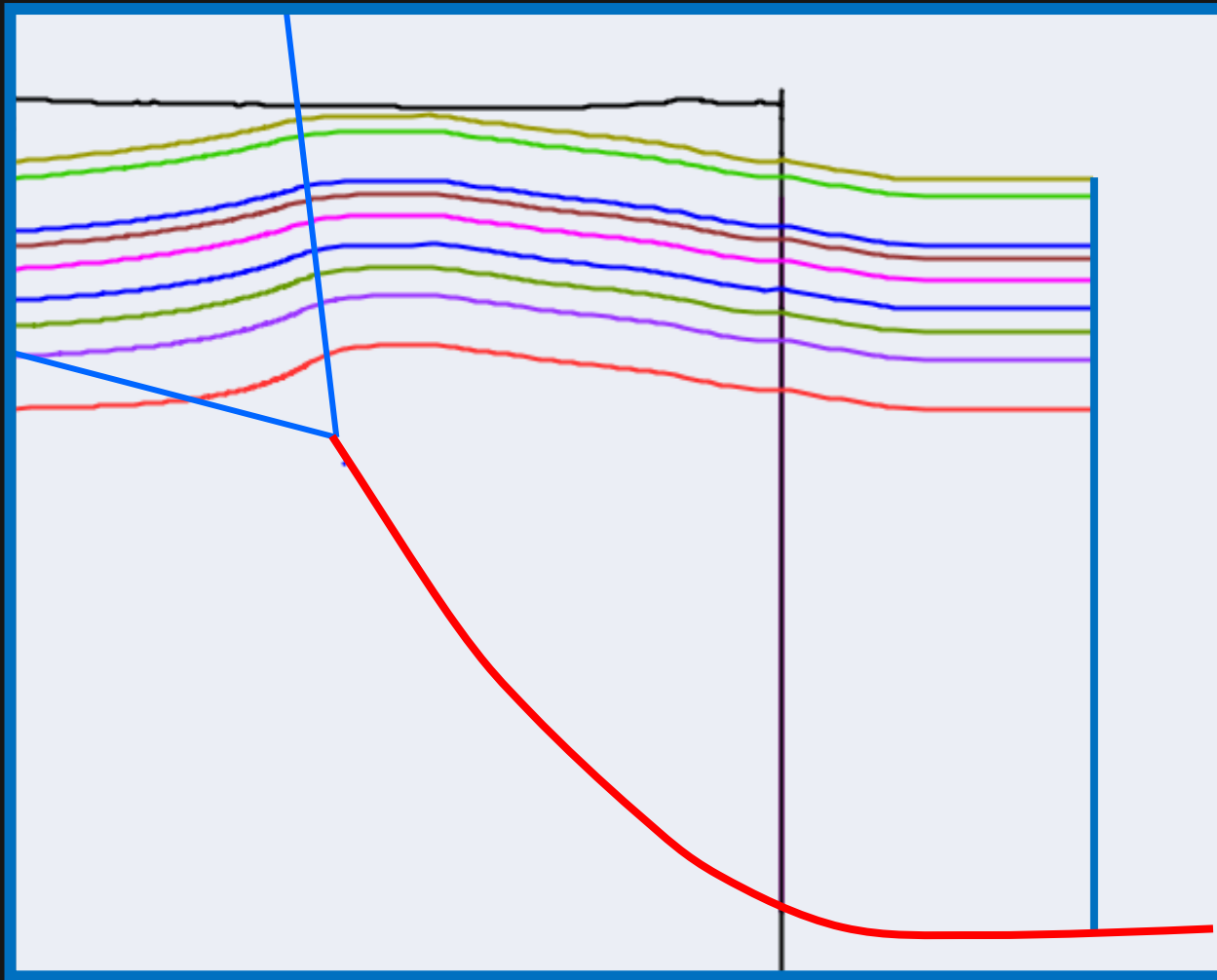
Forward modeling with trishear



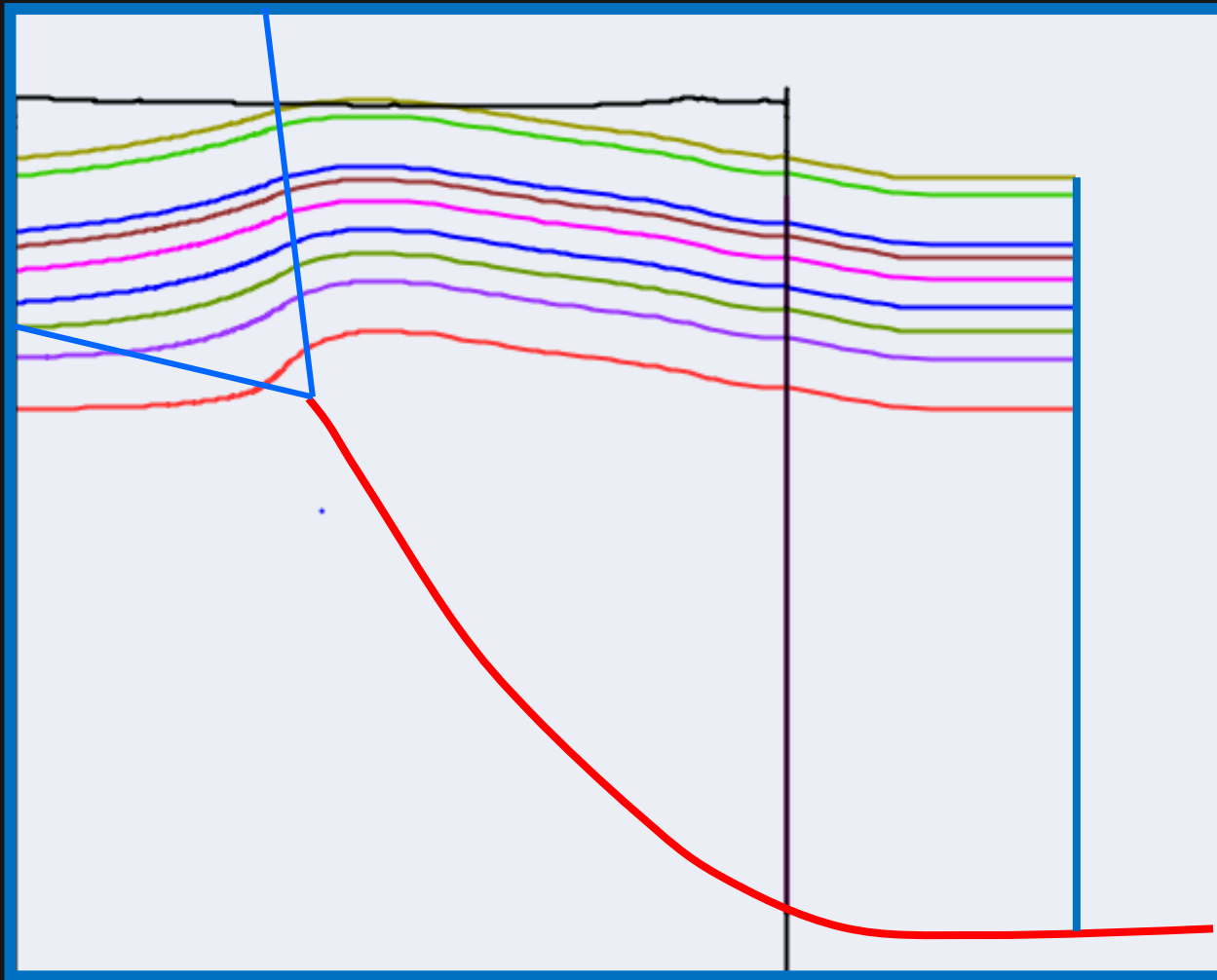
Forward modeling with trishear



Forward modeling with trishear



Forward modeling with trishear



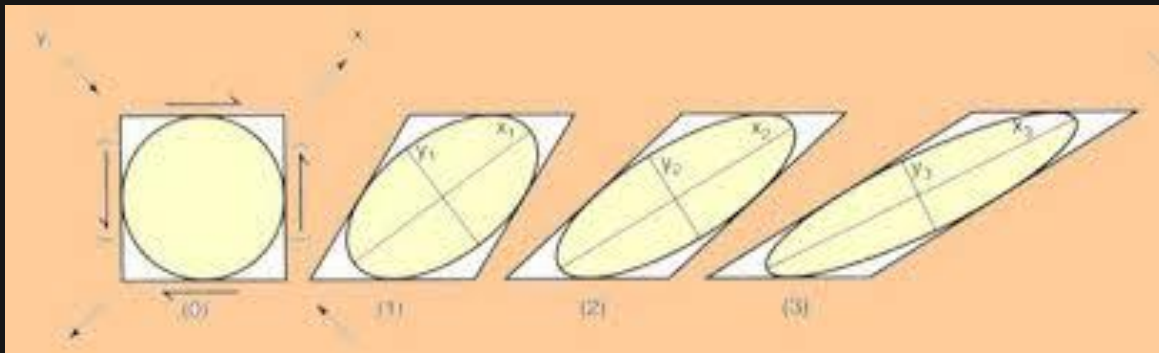
Strain as fracture proxy

Incremental strain = increments of distortion that affect a body during deformation from one stage to the next

Finite strain = summation of all of the incremental components representing the total distortion (strain) compared to its original shape.

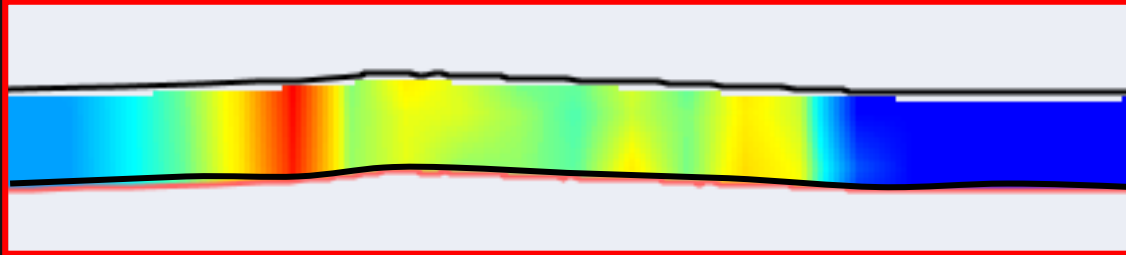
Cumulative strain = summation of all of the incremental components from one step to the next – adding absolute values

HAVE TO KNOW DEFORMATION HISTORY!

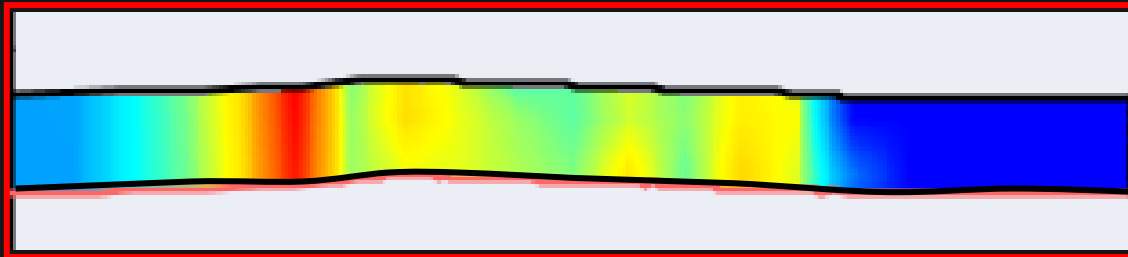


Stages of strain evolution

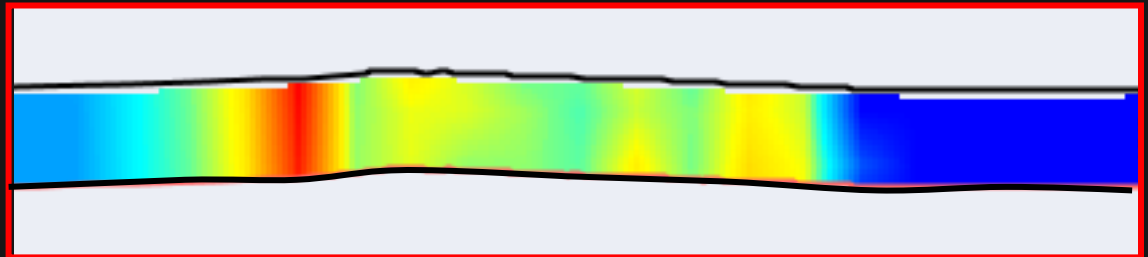
Incremental shear strain



Finite shear strain

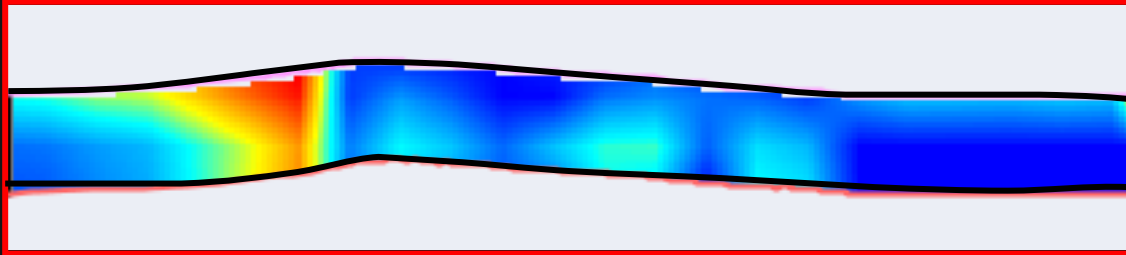


Cumulative shear strain

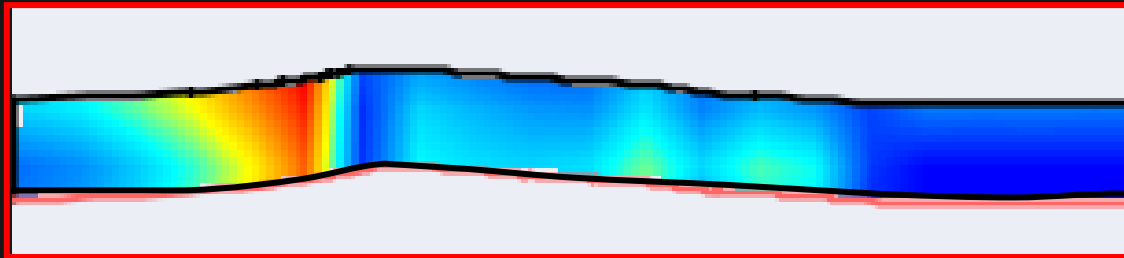


Stages of strain evolution

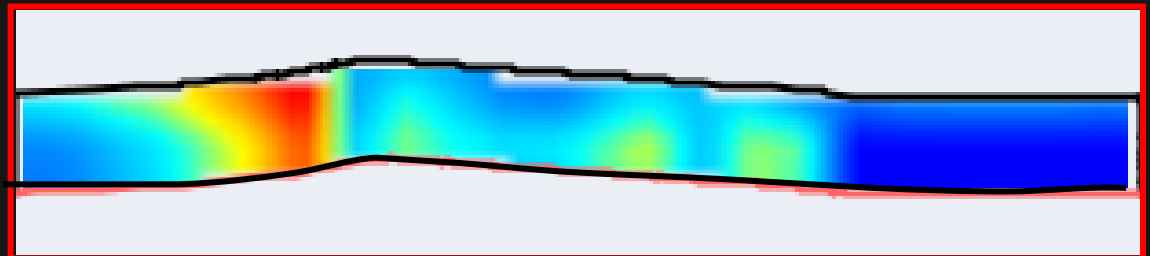
Incremental shear strain



Finite shear strain

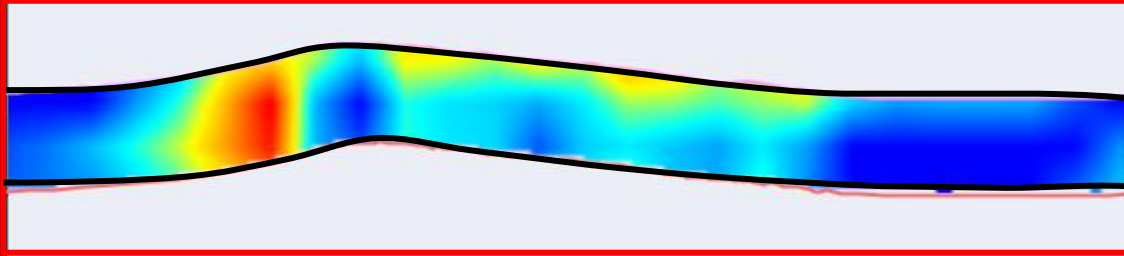


Cumulative shear strain

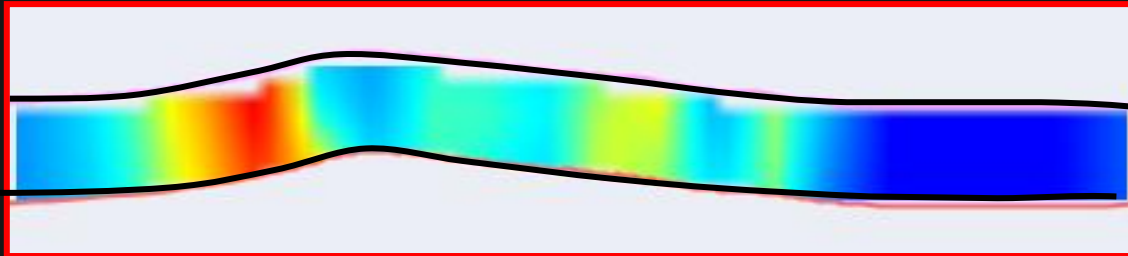


Stages of strain evolution

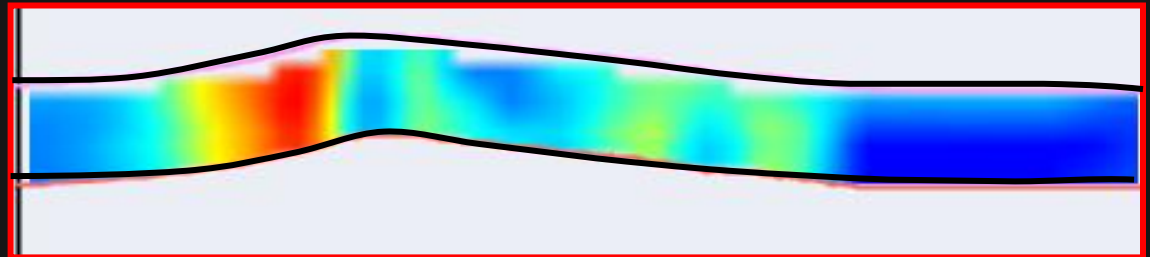
Incremental shear strain



Finite shear strain

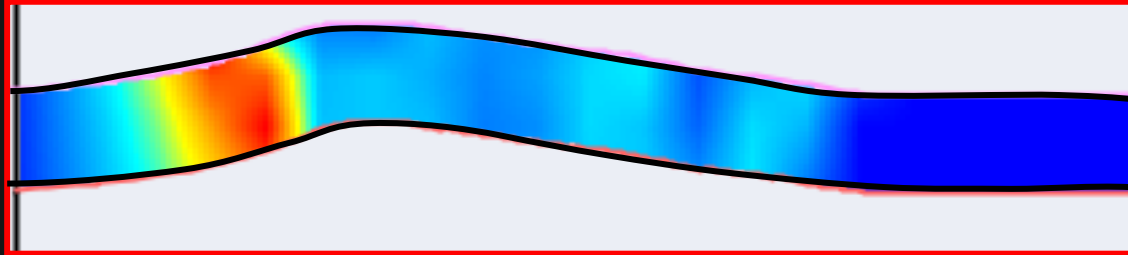


Cumulative shear strain

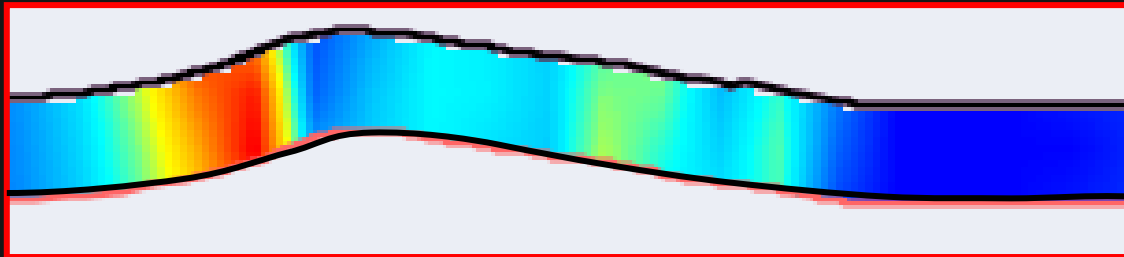


Stages of strain evolution

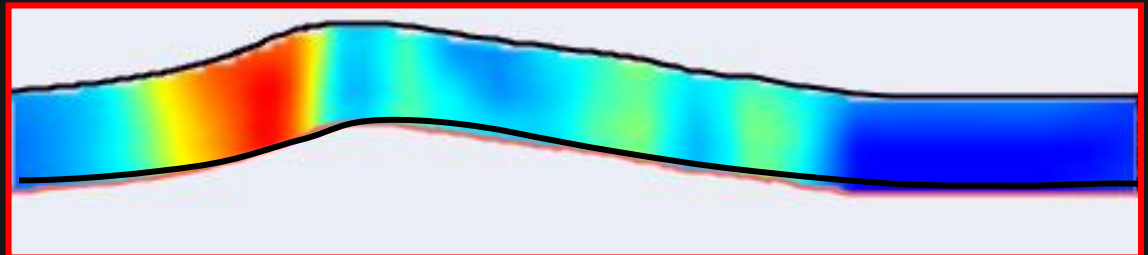
Incremental shear strain



Finite shear strain

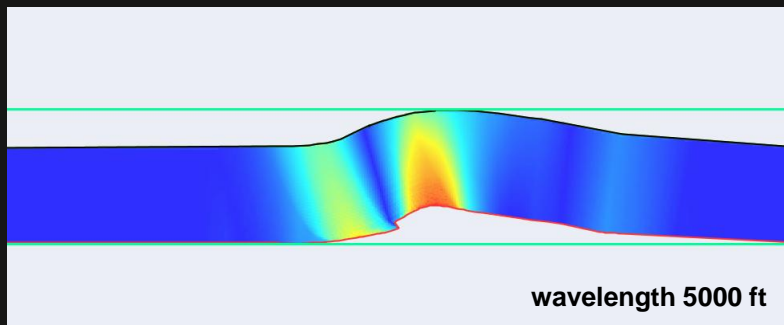
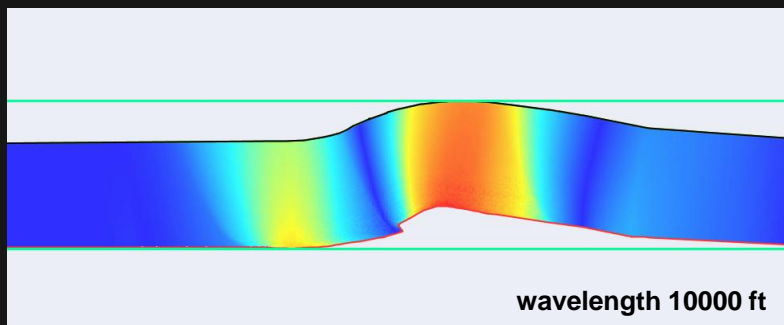
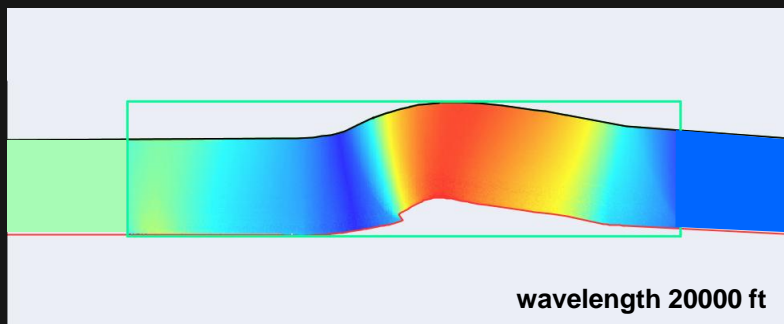


Cumulative shear strain

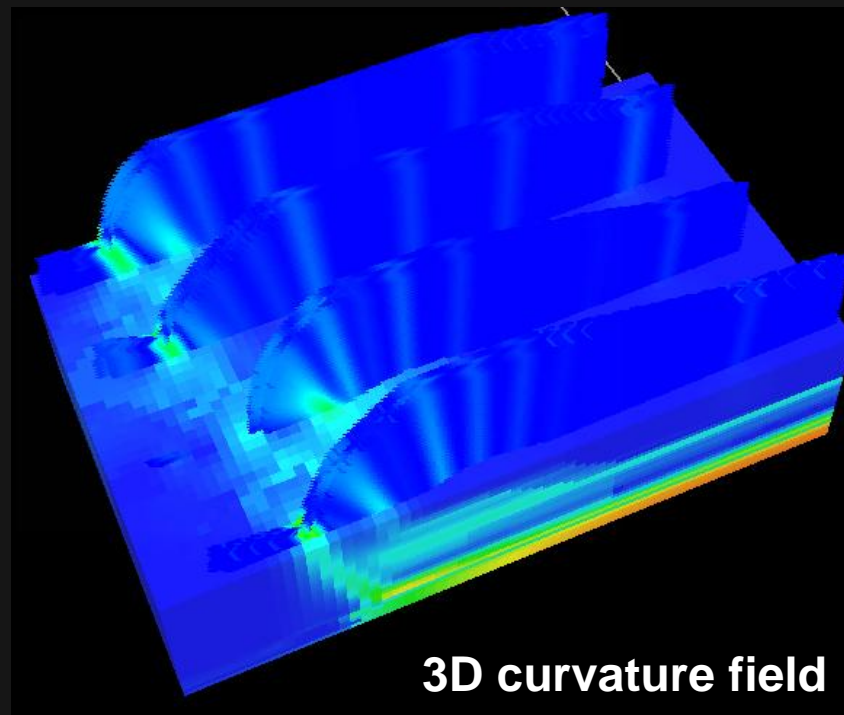
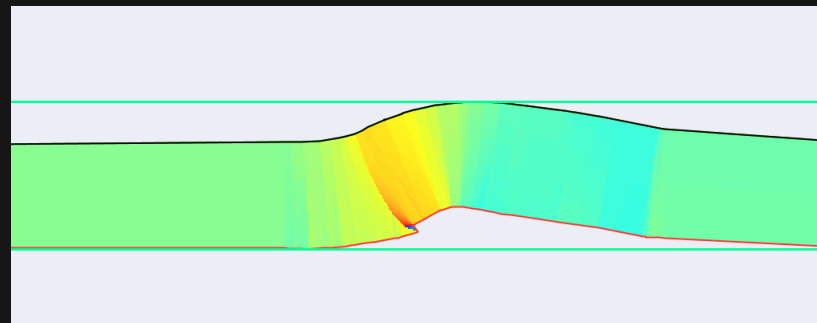


Curvature and dip as fracture proxy

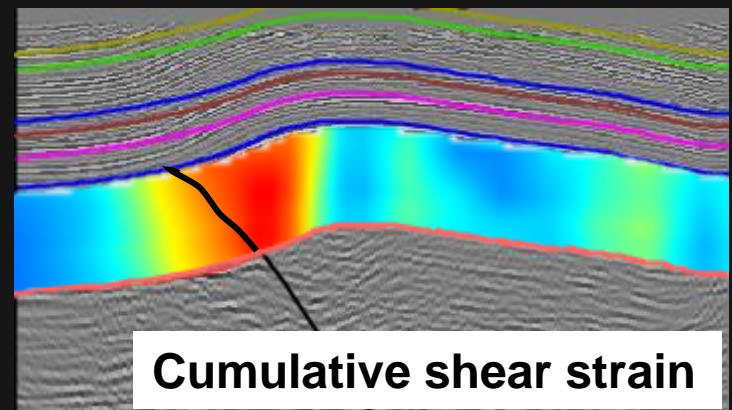
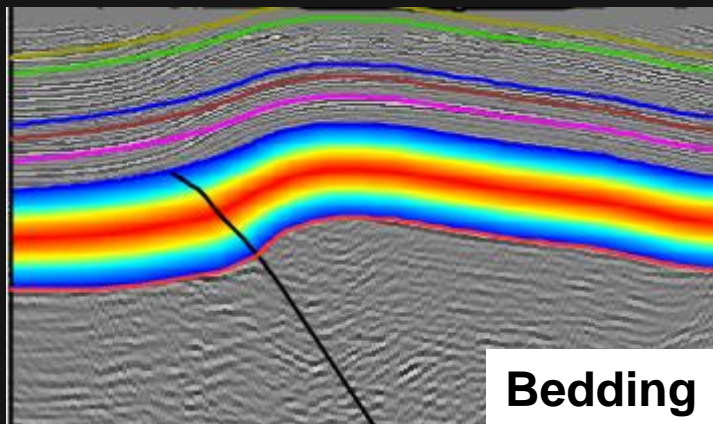
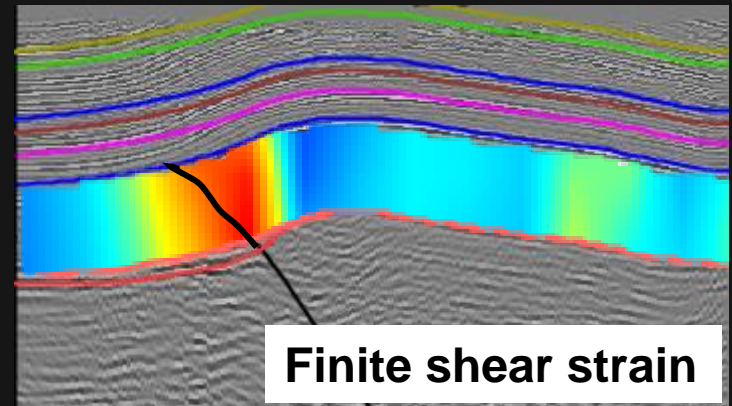
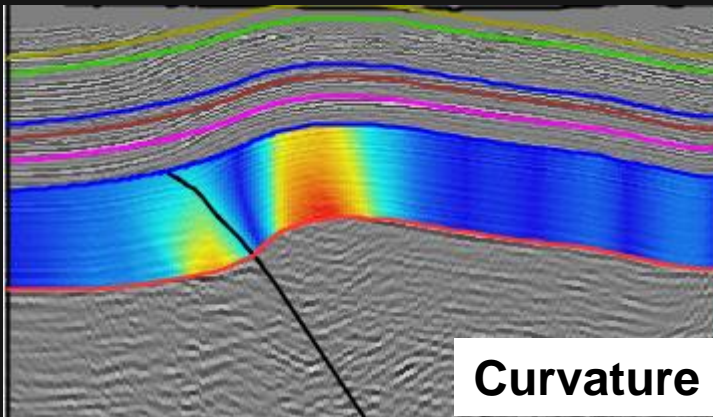
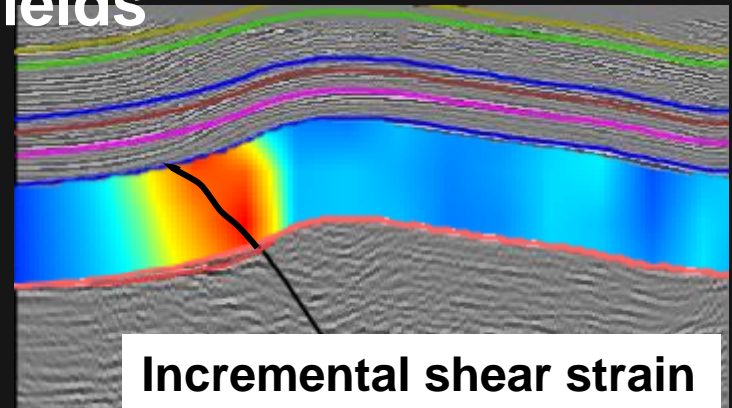
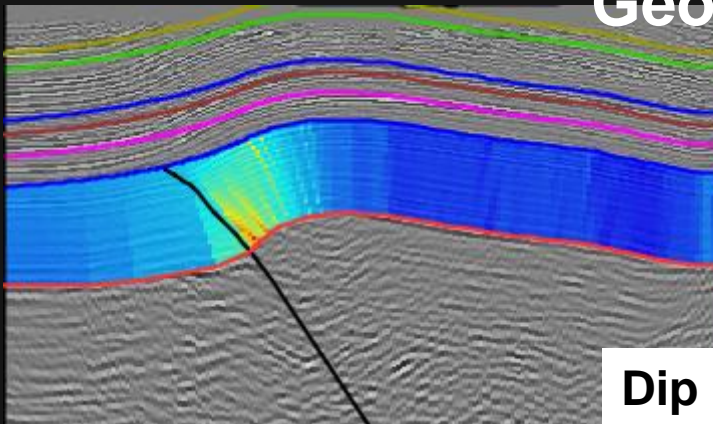
Curvature



Dip



Geometry Fields

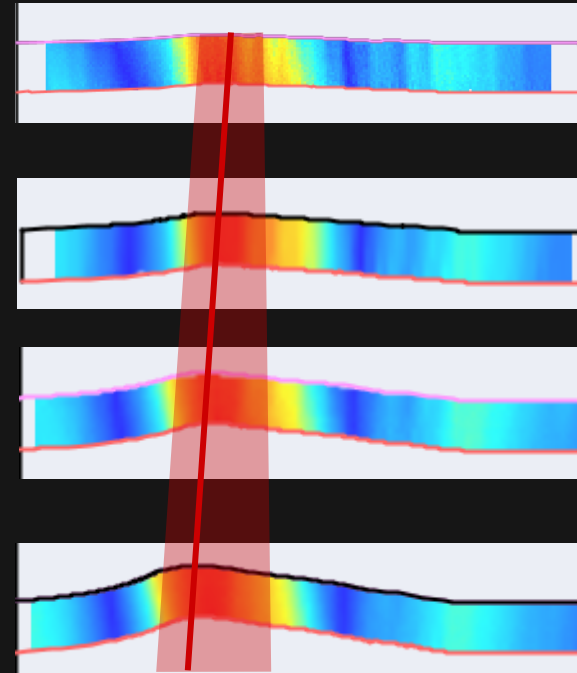
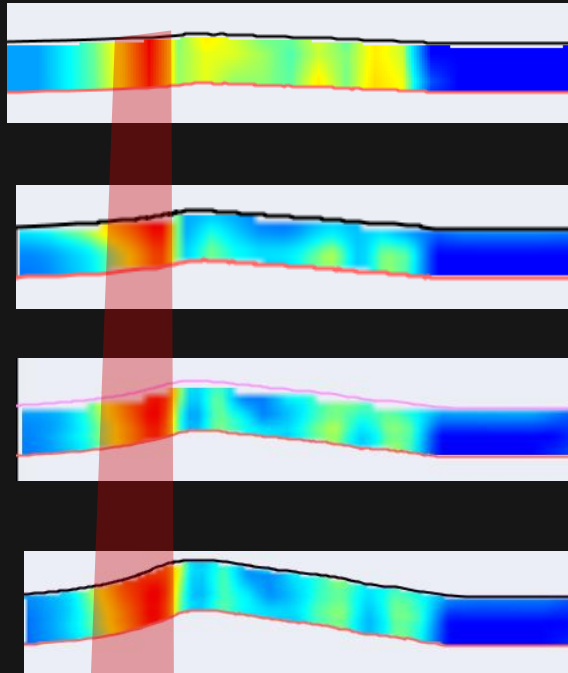
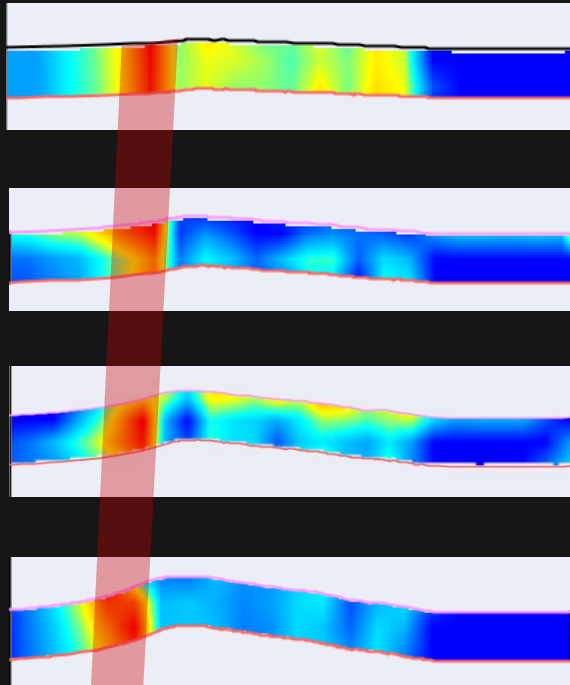


Evolution of strain and curvature

Incremental shear strain

Cumulative shear strain

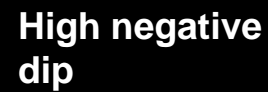
Curvature



Zone of maximum
incremental shear strain
propagates

Zone of maximum
cumulative shear strain
propagates and widens

Zone of max curvature
propagates with hinge
and widens



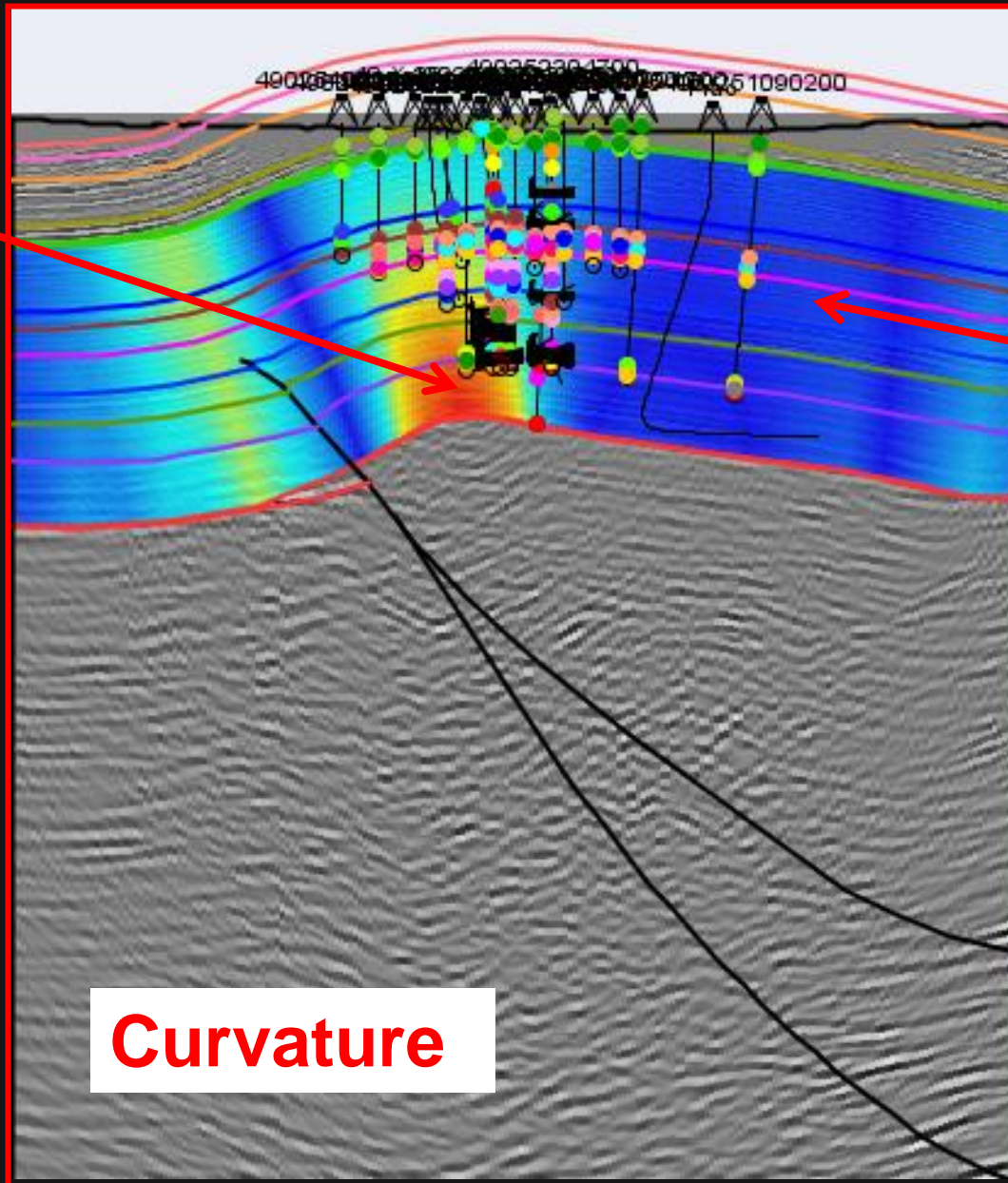
High
curvature

High
curvature

Low
curvature

Curvature

Low min curvature



**Maximum
elongation**

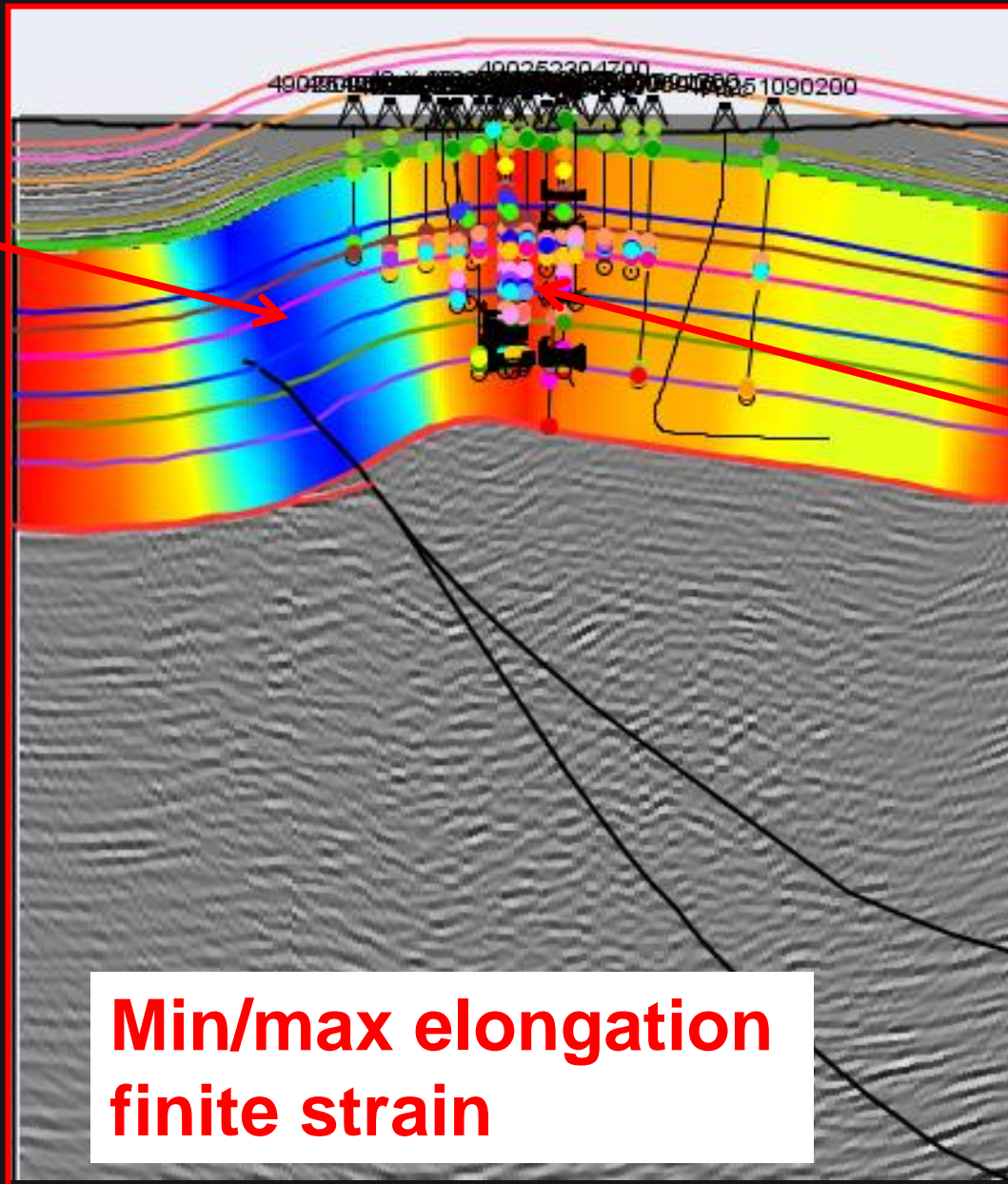
**High min
elongation**

**Minimum
elongation**

**Min/max elongation
finite strain**

**Low min
elongation**

RESERVED.



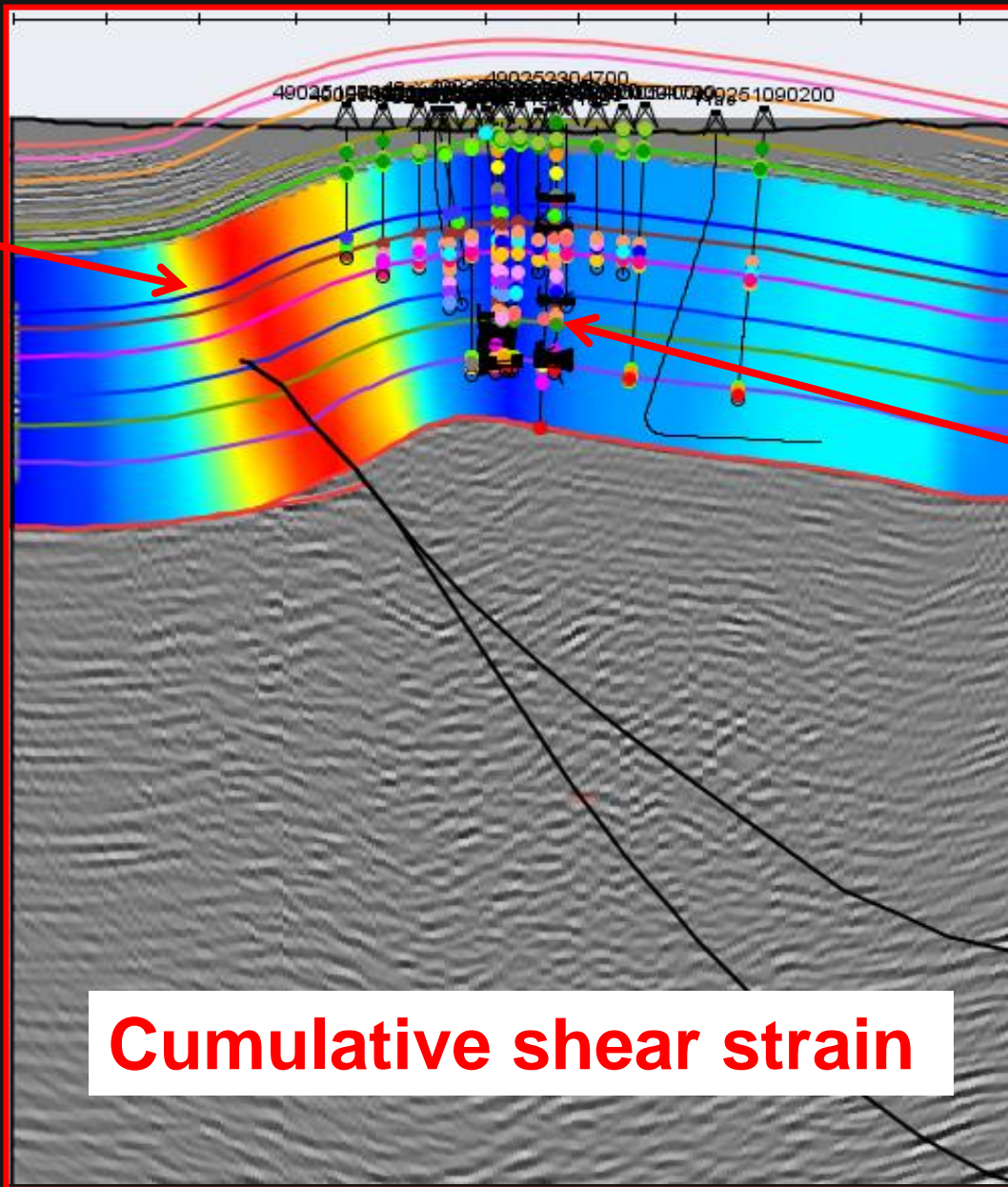
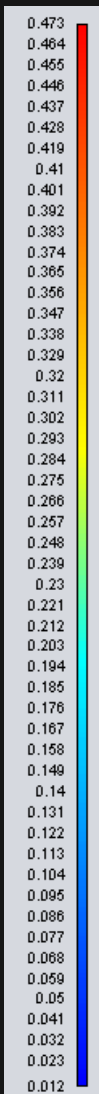
High shear strain

High shear strain


Low shear strain

Cumulative shear strain


RESERVED.




CONCLUSIONS



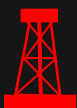
Strain can be used as a proxy for fracture intensity and distribution



Cumulative strain tracks the total rock damage and fracture accumulation



In tight fractured reservoirs fold limbs may be better conduits than fold hinges



Have to calibrate against structural model and folding mechanism
